

An exact conserving algorithm for nonlinear dynamics with rotational DOFs and general hyperelasticity. Part 2: shells

E. M. B. Campello · P. M. Pimenta · P. Wriggers

Received: 2 March 2010 / Accepted: 25 February 2011 / Published online: 30 March 2011
© Springer-Verlag 2011

Abstract Following the approach developed for rods in Part 1 of this paper (Pimenta et al. in *Comput. Mech.* 42:715–732, 2008), this work presents a fully conserving algorithm for the integration of the equations of motion in nonlinear shell dynamics. We begin with a re-parameterization of the rotation field in terms of the so-called Rodrigues rotation vector, allowing for an extremely simple update of the rotational variables within the scheme. The weak form is constructed via non-orthogonal projection, the time-collocation of which ensures exact conservation of momentum and total energy in the absence of external forces. Appealing is the fact that general hyperelastic materials (and not only materials with quadratic potentials) are permitted in a totally consistent way. Spatial discretization is performed using the finite element method and the robust performance of the scheme is demonstrated by means of numerical examples.

Keywords Nonlinear dynamics · Shells · Time integration · Energy conservation · Momentum conservation

1 Introduction

In this work we extend the dynamics formulation developed for nonlinear rods in Part 1 [15] of this paper to the case

E. M. B. Campello · P. M. Pimenta (✉)
Polytechnic School at the University of São Paulo,
P.O. Box 61548, 05424-970 São Paulo, Brazil
e-mail: ppimenta@usp.br

E. M. B. Campello
e-mail: campello@usp.br

P. Wriggers
Institute for Continuum Mechanics, Leibniz Universität Hannover,
Appelstrasse 11, 30167 Hanover, Germany
e-mail: wriggers@ikm.uni-hannover.de

of nonlinear shells. A fully conserving algorithm for integration of the resulting equations of motion is attained, with the remarkable property of allowing for general hyperelastic materials.

As a consequence of our notation, the expressions derived are virtually identical to the corresponding ones of the rod model. This feature illustrates the profound connection between the two papers and leads to a straightforward implementation of the shell formulation within a finite element code once the rod model has been implemented.

As in Part 1, our starting point is a re-parameterization of the rotation field in terms of the so-called Rodrigues rotation vector (see [14]), with which update of the rotational variables is made extremely simple within the scheme. The geometrically-exact quasi-static shell model of [5, 12] is adopted as the basis for our developments. Energetically conjugated cross-sectional stresses and strains are defined based upon the first Piola–Kirchhoff stress tensor and the deformation gradient. The equations of motion are derived in an exact manner and the corresponding weak form is constructed via non-orthogonal projection, equivalent to the application of the virtual power theorem. Time-collocation of the resulting expressions following an energy-momentum approach ensures exact conservation of both momentum and mechanical energy in the absence of external forces. Spatial discretization is performed under the light of the finite element method and the performance of the scheme is assessed by means of several numerical simulations.

We draw the attention of the reader to the fact that, up to our knowledge, this is the first conserving scheme as to permit general hyperelastic materials in the dynamics of nonlinear shells with rotational degrees-of-freedom. For a brief overview and historical notes on the subject, we refer to the introduction in Part 1 of this paper.

Throughout the text, italic Greek or Latin lowercase letters ($a, b, \dots, \alpha, \beta, \dots$) denote scalar quantities, bold italic Greek or Latin lowercase letters ($\mathbf{a}, \mathbf{b}, \dots, \boldsymbol{\alpha}, \boldsymbol{\beta}, \dots$) denote vectors and bold italic Greek or Latin capital letters ($\mathbf{A}, \mathbf{B}, \dots$) denote second-order tensors in a three-dimensional Euclidean space. Summation convention over repeated indices is adopted, with Greek indices ranging from 1 to 2 and Latin indices from 1 to 3.

2 Parameterization of the rotation field

Following the parameterization developed for the rotation field in [15], let $\boldsymbol{\theta}$ be the classical Euler rotation vector representing an arbitrary finite rotation on 3-D space, with $\theta = \|\boldsymbol{\theta}\|$ as its magnitude and

$$\mathbf{Q} = \mathbf{I} + \frac{\sin \theta}{\theta} \boldsymbol{\Theta} + \frac{1}{2} \left(\frac{\sin \theta/2}{\theta/2} \right)^2 \boldsymbol{\Theta}^2 \tag{1}$$

as the associated rotation tensor, in which $\boldsymbol{\Theta} = \text{Skew}(\boldsymbol{\theta})$. We define the Rodrigues rotation vector $\boldsymbol{\alpha}$ by means of

$$\boldsymbol{\alpha} = \frac{\tan(\theta/2)}{\theta/2} \boldsymbol{\theta}, \tag{2}$$

and opt to describe the rotation field with $\boldsymbol{\alpha}$ instead of $\boldsymbol{\theta}$. The rotation tensor may be expressed in terms of $\boldsymbol{\alpha}$ as follows (see [14])

$$\mathbf{Q} = \mathbf{I} + h(\alpha) \left(\mathbf{A} + \frac{1}{2} \mathbf{A}^2 \right), \quad \text{with } h(\alpha) = \frac{4}{4 + \alpha^2}, \tag{3}$$

where $\alpha = \|\boldsymbol{\alpha}\|$ and $\mathbf{A} = \text{Skew}(\boldsymbol{\alpha})$. In this case, the Cayley transform

$$\mathbf{Q} = \left(\mathbf{I} + \frac{1}{2} \mathbf{A} \right) \left(\mathbf{I} - \frac{1}{2} \mathbf{A} \right)^{-1} = \left(\mathbf{I} - \frac{1}{2} \mathbf{A} \right)^{-1} \left(\mathbf{I} + \frac{1}{2} \mathbf{A} \right) \tag{4}$$

holds for \mathbf{Q} , and the following relations may be derived:

$$\begin{aligned} \frac{1}{2}(\mathbf{I} + \mathbf{Q}) &= \left(\mathbf{I} - \frac{1}{2} \mathbf{A} \right)^{-1} \\ \text{and } \mathbf{Q} - \mathbf{I} &= \mathbf{A} \left(\mathbf{I} - \frac{1}{2} \mathbf{A} \right)^{-1} = \left(\mathbf{I} - \frac{1}{2} \mathbf{A} \right)^{-1} \mathbf{A}. \end{aligned} \tag{5}$$

The skew-symmetric spin tensor associated to the rotation \mathbf{Q} is defined by $\boldsymbol{\Omega} = \dot{\mathbf{Q}}\mathbf{Q}^T$, with its axial vector $\boldsymbol{\omega} = \text{axial}(\boldsymbol{\Omega})$ being called the spin vector or angular velocity vector. One can show that

$$\boldsymbol{\omega} = \boldsymbol{\Xi} \dot{\boldsymbol{\alpha}}, \quad \text{where } \boldsymbol{\Xi} = h(\alpha) \left(\mathbf{I} + \frac{1}{2} \mathbf{A} \right). \tag{6}$$

Tensor $\boldsymbol{\Xi}$ therefore relates $\boldsymbol{\omega}$ to the time derivative of $\boldsymbol{\alpha}$ and has the remarkable property $\mathbf{Q}^T \boldsymbol{\Xi} \mathbf{Q} = \boldsymbol{\Xi}$, from which follows $\boldsymbol{\Xi}^T = \mathbf{Q}^T \boldsymbol{\Xi} = \boldsymbol{\Xi} \mathbf{Q}^T$. From these identities, the back-rotated counterpart of $\boldsymbol{\omega}$ is given by

$$\boldsymbol{\omega}^r = \mathbf{Q}^T \boldsymbol{\omega} = \boldsymbol{\Xi}^T \dot{\boldsymbol{\alpha}}, \tag{7}$$

where the notation with a superscript “ r ” was introduced to define back-rotated quantities.

Let now \mathbf{t} be a generic vector and \mathbf{T} a second-order tensor such that $\mathbf{T} = \text{Skew}(\mathbf{t})$. The following result (useful subsequently in the text) may be obtained by differentiation

$$\begin{aligned} \frac{\partial(\boldsymbol{\Xi}^T \mathbf{t})}{\partial \boldsymbol{\alpha}} &= \mathbf{W}(\boldsymbol{\alpha}, \mathbf{t}), \\ \text{where } \mathbf{W}(\boldsymbol{\alpha}, \mathbf{t}) &= \frac{1}{2} h(\alpha) (\mathbf{T} - \boldsymbol{\Xi}^T \mathbf{t} \otimes \boldsymbol{\alpha}). \end{aligned} \tag{8}$$

Other useful properties are

$$\begin{aligned} \det(\boldsymbol{\Xi}) &= h^2(\alpha), \quad \det \left[\frac{1}{2}(\mathbf{I} + \mathbf{Q}) \right] = h(\alpha), \\ \boldsymbol{\Xi} &= \det \left[\frac{1}{2}(\mathbf{I} + \mathbf{Q}) \right] \left[\frac{1}{2}(\mathbf{I} + \mathbf{Q}) \right]^{-T} = h(\alpha) \left[\frac{1}{2}(\mathbf{I} + \mathbf{Q}) \right]^{-T} \\ \text{and } \left[\frac{1}{2}(\mathbf{I} + \mathbf{Q}) \mathbf{a} \right] \times \left[\frac{1}{2}(\mathbf{I} + \mathbf{Q}) \mathbf{b} \right] &= \boldsymbol{\Xi}(\mathbf{a} \times \mathbf{b}), \\ \forall \mathbf{a}, \mathbf{b} \in \mathbb{R}^3 & \quad (\text{Nanson's rule}). \end{aligned} \tag{9}$$

The parameterization with the Rodrigues rotation vector leads to simpler expressions when compared to the Euler representation, and allows for a very simple update scheme of the rotation field as we shall see subsequently. It should be mentioned, however, that due to definition (2) we must have $0 < \theta < \pi$. This restriction does not affect the algorithm since we will use an updated formulation. Hence, the rotations may not exceed π only within a single time increment, what may not be considered a practical limitation.

3 Shell dynamics

3.1 Kinematics

Based on the geometrically-exact quasi-static shell model of [5, 12], a flat reference configuration is assumed for the shell mid-surface at the outset. A local orthonormal system $\{\mathbf{e}_1^r, \mathbf{e}_2^r, \mathbf{e}_3^r\}$ with corresponding coordinates $\{\xi_1, \xi_2, \zeta\}$ is defined at this configuration, with vectors \mathbf{e}_α^r placed on the shell mid-plane and \mathbf{e}_3^r normal to it (see Fig. 1). Points in this configuration are described by

$$\boldsymbol{\xi} = \boldsymbol{\zeta} + \mathbf{r}^r, \tag{10}$$

where $\boldsymbol{\zeta} = \xi_\alpha \mathbf{e}_\alpha^r$ describes the position of points on the mid-surface and $\mathbf{r}^r = \zeta \mathbf{e}_3^r$ is the reference director, with $\zeta \in H = [-h^b, h^t]$ as the thickness coordinate and $h = h^t + h^b$ as the shell reference thickness.

Let now $\{\mathbf{e}_1, \mathbf{e}_2, \mathbf{e}_3\}$ be a local orthonormal system in the current configuration as depicted in Fig. 1, with \mathbf{e}_3 aligned with the current director and \mathbf{e}_α normal to it. We describe the shell motion by a vector field $\mathbf{x} = \hat{\mathbf{x}}(\boldsymbol{\xi})$, so that in this configuration the position of the material points is given by

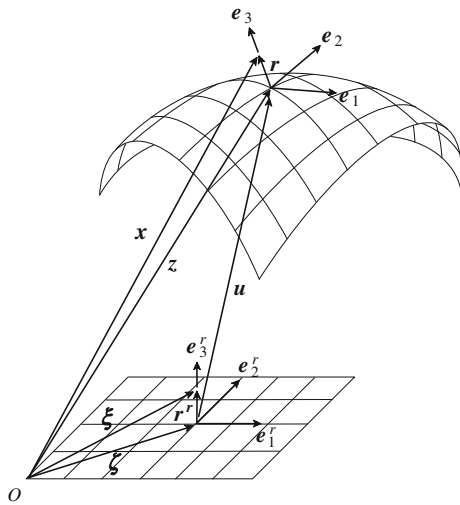


Fig. 1 Shell description and basic kinematical quantities

$$x = z + r, \tag{11}$$

where

$$z = \zeta + u \tag{12}$$

describes the position of points in the mid-surface (with u as the displacement vector) and

$$r = Qr^r \tag{13}$$

is the current director at these points, with Q as the rotation tensor given by Eq. (3). Notice that expression (13) embeds our basic kinematical assumption, i.e. the director remains undeformed during the shell motion (no thickness changes occur) and may only rotate as a rigid body, with first-order shear deformations being accounted for. Relation $e_i = Qe_i^r$ holds for the local systems.

Time differentiation of expression (11) furnishes the velocity and acceleration vectors of a material point:

$$\dot{x} = \dot{u} + \omega \times r \quad \text{and} \quad \ddot{x} = \dot{u} + \dot{\omega} \times r + \omega \times (\omega \times r). \tag{14}$$

3.2 Strains

The deformation gradient F is computed by differentiation of (11) with respect to ξ , and after some algebra can be expressed by

$$F = Q[I + (\eta_\alpha^r + \kappa_\alpha^r \times r^r) \otimes e_\alpha^r], \tag{15}$$

where

$$\begin{aligned} \eta_\alpha^r &= Q^T z_{,\alpha} - e_\alpha^r \quad \text{and} \\ \kappa_\alpha^r &= Q^T \text{axial}(Q_{,\alpha} Q^T) = \Xi^T \alpha_{,\alpha} \end{aligned} \tag{16}$$

may be regarded as the shell strain vectors [notation $(\cdot)_{,\alpha} = \partial(\cdot)/\partial\xi_\alpha$ was introduced in (16)]. Time differentiation of the above expressions provides the strain rate vectors as follows

$$\begin{aligned} \dot{\eta}_\alpha^r &= Q^T (\dot{u}_{,\alpha} + z_{,\alpha} \times \omega) = Q^T (\dot{u}_{,\alpha} + Z_{,\alpha} \Xi \dot{\alpha}) \quad \text{and} \\ \dot{\kappa}_\alpha^r &= Q^T \omega_{,\alpha} = \Xi^T \dot{\alpha}_{,\alpha} + \dot{\Xi}^T \alpha_{,\alpha} \\ &= Q^T [\Xi \dot{\alpha}_{,\alpha} + QW(\alpha, \alpha_{,\alpha}) \dot{\alpha}], \end{aligned} \tag{17}$$

with $W(\alpha, \alpha_{,\alpha})$ as in (8). If we place η_α^r and κ_α^r within a generalized strain vector ϵ_α^r , i.e.

$$\epsilon_\alpha^r = \begin{bmatrix} \eta_\alpha^r \\ \kappa_\alpha^r \end{bmatrix}, \tag{18}$$

then the generalized strain rate $\dot{\epsilon}_\alpha^r$ may be written as [with the aid of (17)]

$$\dot{\epsilon}_\alpha^r = \Lambda^T \Phi_\alpha \Delta_\alpha v, \tag{19}$$

where

$$\begin{aligned} \Lambda &= \begin{bmatrix} Q & O \\ O & Q \end{bmatrix}, \quad \Phi_\alpha = \begin{bmatrix} I & O & Z_{,\alpha} \\ O & I & O \end{bmatrix}, \\ \Delta_\alpha &= \begin{bmatrix} I \frac{\partial}{\partial \xi_\alpha} & O \\ O & I \frac{\partial}{\partial \xi_\alpha} \\ O & I \end{bmatrix} \quad \text{and} \quad v = \begin{bmatrix} \dot{u} \\ \omega \end{bmatrix}. \end{aligned} \tag{20}$$

In addition, if we define an operator Y_α and a vector d such that

$$\begin{aligned} \Delta_\alpha v &= Y_\alpha \Delta_\alpha \dot{d}, \quad \text{where} \quad Y_\alpha = \begin{bmatrix} I & O & O \\ O & \Xi & QW(\alpha, \alpha_{,\alpha}) \\ O & O & \Xi \end{bmatrix} \\ \text{and} \quad d &= \begin{bmatrix} u \\ \alpha \end{bmatrix}, \end{aligned} \tag{21}$$

then it is possible to rewrite (19) as

$$\dot{\epsilon}_\alpha^r = \Lambda^T \Phi_\alpha Y_\alpha \Delta_\alpha \dot{d}. \tag{22}$$

3.3 Stresses

Let the first Piola–Kirchhoff stress tensor be expressed in terms of its column-vectors by

$$P = \tau_i \otimes e_i^r, \tag{23}$$

where τ_i are nominal stress vectors acting on points of the shell at the current configuration whose normal vectors at the reference configuration are e_i^r . Since e_α^r are the normal vectors to the undeformed cross-sections, τ_α correspond to the cross-sectional stress vectors. Integration of τ_α over the shell reference thickness furnishes the stress resultants as below

$$n_\alpha = \int_H \tau_\alpha dH \quad \text{and} \quad m_\alpha = \int_H r \times \tau_\alpha dH, \tag{24}$$

which stand for the internal forces and internal moments acting on the cross-sections, respectively, both per unit length

of the reference configuration. Considering the back-rotated stress vectors $\tau_i^r = \mathbf{Q}^T \tau_i$, the back-rotated counterparts of (24) may be written as

$$\begin{aligned} \mathbf{n}_\alpha^r &= \mathbf{Q}^T \mathbf{n}_\alpha = \int_H \tau_\alpha^r dH \quad \text{and} \quad \mathbf{m}_\alpha^r = \mathbf{Q}^T \mathbf{m}_\alpha \\ &= \int_H \mathbf{r}^r \times \tau_\alpha^r dH. \end{aligned} \tag{25}$$

For the sake of compactness in notation, we will place these resultants into the vectors below

$$\boldsymbol{\sigma}_\alpha = \begin{bmatrix} \mathbf{n}_\alpha \\ \mathbf{m}_\alpha \end{bmatrix} \quad \text{and} \quad \boldsymbol{\sigma}_\alpha^r = \begin{bmatrix} \mathbf{n}_\alpha^r \\ \mathbf{m}_\alpha^r \end{bmatrix}. \tag{26}$$

Note that $\boldsymbol{\sigma}_\alpha^r = \mathbf{A}^T \boldsymbol{\sigma}_\alpha$ and $\boldsymbol{\sigma}_\alpha = \mathbf{A} \boldsymbol{\sigma}_\alpha^r$, with \mathbf{A} given in (20)₁.

3.4 External forces

Let $\bar{\mathbf{n}}$ be the applied external forces and $\bar{\mathbf{m}}$ the applied external moments acting on the shell mid-surface both by unit area of the reference configuration. Let $\bar{\mathbf{n}}^\Gamma$ be the external distributed forces and $\bar{\mathbf{m}}^\Gamma$ the external distributed moments acting on the shell edges by unit length of the reference configuration. The resulting external forces and moments on the shell are then given by

$$\begin{aligned} \mathbf{f}^{\text{ext}} &= \int_\Omega \bar{\mathbf{n}} d\Omega + \int_\Gamma \bar{\mathbf{n}}^\Gamma d\Gamma \quad \text{and} \\ \mathbf{m}^{\text{ext}} &= \int_\Omega (\mathbf{z} \times \bar{\mathbf{n}} + \bar{\mathbf{m}}) d\Omega + \int_\Gamma (\mathbf{z} \times \bar{\mathbf{n}}^\Gamma + \bar{\mathbf{m}}^\Gamma) d\Gamma, \end{aligned} \tag{27}$$

in which $\Omega \subset \mathbb{R}^2$ is the shell (open) domain and $\Gamma = \partial\Omega$ is its boundary (notice that the external moments are defined with respect to the origin of the coordinates).

3.5 Linear and angular momentum

Let ρ be the specific mass of the shell at the reference configuration and assume for simplicity that the shell mid-surface is the medium surface, i.e. $H = [-h/2, h/2]$, such that

$$\int_H \rho \mathbf{r}^r dH = \int_H \rho \mathbf{r} dH = \mathbf{o}. \tag{28}$$

We then define the following inertia properties for the cross-sections:

$$\begin{aligned} \bar{\mathbf{M}} &= \int_H \rho dH \quad \text{and} \\ \bar{\mathbf{J}} &= - \int_H \text{Skew}^2(\mathbf{r}) \rho dH, \\ \bar{\mathbf{J}}^r &= - \int_H \text{Skew}^2(\mathbf{r}^r) \rho dH = \mathbf{Q}^T \bar{\mathbf{J}} \mathbf{Q}. \end{aligned} \tag{29}$$

Let now V be the volume at the reference configuration. The linear momentum of the shell [with the aid of (14)₁] is given by

$$\boldsymbol{\lambda} = \int_V \rho \dot{\mathbf{x}} dV = \int_\Omega \bar{\boldsymbol{\lambda}} d\Omega, \quad \text{where} \quad \bar{\boldsymbol{\lambda}} = \bar{\mathbf{M}} \dot{\mathbf{u}}, \tag{30}$$

and the angular momentum [with the aid of (11) and (14)₁] by

$$\begin{aligned} \boldsymbol{\mu} &= \int_V \rho \mathbf{x} \times \dot{\mathbf{x}} dV = \int_\Omega (\mathbf{z} \times \bar{\boldsymbol{\lambda}} + \bar{\boldsymbol{\mu}}) d\Omega, \quad \text{where} \\ \bar{\boldsymbol{\mu}} &= \bar{\mathbf{J}} \boldsymbol{\omega} = \mathbf{Q} \bar{\boldsymbol{\mu}}^r \quad \text{and} \quad \bar{\boldsymbol{\mu}}^r = \bar{\mathbf{J}}^r \boldsymbol{\omega}^r. \end{aligned} \tag{31}$$

Notice that the angular momentum $\boldsymbol{\mu}$ is defined here with respect to the origin of the coordinates. Time differentiation of $\boldsymbol{\lambda}$ and $\boldsymbol{\mu}$ results in

$$\begin{aligned} \dot{\boldsymbol{\lambda}} &= \int_\Omega \dot{\bar{\boldsymbol{\lambda}}} d\Omega, \quad \text{with} \quad \dot{\bar{\boldsymbol{\lambda}}} = \bar{\mathbf{M}} \ddot{\mathbf{u}}, \quad \text{and} \\ \dot{\boldsymbol{\mu}} &= \int_\Omega (\mathbf{z} \times \dot{\bar{\boldsymbol{\lambda}}} + \dot{\bar{\boldsymbol{\mu}}}) d\Omega, \quad \text{with} \quad \dot{\bar{\boldsymbol{\mu}}} = \bar{\mathbf{J}} \dot{\boldsymbol{\omega}} + \boldsymbol{\omega} \times \bar{\mathbf{J}} \boldsymbol{\omega} = \mathbf{Q} \dot{\bar{\boldsymbol{\mu}}}^r \\ \text{and} \quad \dot{\bar{\boldsymbol{\mu}}}^r &= \bar{\mathbf{J}}^r \dot{\boldsymbol{\omega}}^r + \boldsymbol{\omega}^r \times \bar{\mathbf{J}}^r \boldsymbol{\omega}^r. \end{aligned} \tag{32}$$

We remark that $\dot{\bar{\boldsymbol{\mu}}}^r = (\dot{\bar{\boldsymbol{\mu}}})^r \neq (\bar{\boldsymbol{\mu}}^r)^\cdot$, since $\bar{\boldsymbol{\mu}}^r = \mathbf{Q}^T \bar{\boldsymbol{\mu}}$ and $\dot{\bar{\boldsymbol{\mu}}}^r = (\bar{\boldsymbol{\mu}}^r)^\cdot + \boldsymbol{\omega}^r \times \bar{\boldsymbol{\mu}}^r$.

3.6 Shell equations of motion

The global equations of motion describing the shell dynamics may be stated by means of the Euler’s laws, i.e.

$$\mathbf{f}^{\text{ext}} = \dot{\boldsymbol{\lambda}} \quad \text{and} \quad \mathbf{m}^{\text{ext}} = \dot{\boldsymbol{\mu}}. \tag{33}$$

Substituting (27) and (32) into these two expressions renders

$$\begin{aligned} \int_\Omega (\bar{\mathbf{n}} - \dot{\bar{\boldsymbol{\lambda}}}) d\Omega + \int_\Gamma \bar{\mathbf{n}}^\Gamma d\Gamma &= \mathbf{o} \quad \text{and} \\ \int_\Omega (\mathbf{z} \times \bar{\mathbf{n}} + \bar{\mathbf{m}} - \mathbf{z} \times \dot{\bar{\boldsymbol{\lambda}}} - \dot{\bar{\boldsymbol{\mu}}}) d\Omega \\ + \int_\Gamma (\mathbf{z} \times \bar{\mathbf{n}}^\Gamma + \bar{\mathbf{m}}^\Gamma) d\Gamma &= \mathbf{o}. \end{aligned} \tag{34}$$

On the other hand, from application of the divergence theorem on the cross-sectional resultants \mathbf{n}_α and \mathbf{m}_α , we may write

$$\int_\Omega \mathbf{n}_{\alpha,\alpha} d\Omega = \int_\Gamma \mathbf{n}^\Gamma d\Gamma, \quad \int_\Omega \mathbf{m}_{\alpha,\alpha} d\Omega = \int_\Gamma \mathbf{m}^\Gamma d\Gamma \quad \text{and}$$

$$\int_\Omega (\mathbf{z} \times \mathbf{n}_\alpha)_{,\alpha} d\Omega = \int_\Omega (\mathbf{z}_{,\alpha} \times \mathbf{n}_\alpha + \mathbf{z} \times \mathbf{n}_{\alpha,\alpha}) d\Omega$$

$$= \int_\Gamma (\mathbf{z} \times \mathbf{n}^\Gamma) d\Gamma, \tag{35}$$

where

$$\mathbf{n}^\Gamma = \nu_\alpha \mathbf{n}_\alpha \quad \text{and}$$

$$\mathbf{m}^\Gamma = \nu_\alpha \mathbf{m}_\alpha \tag{36}$$

may be regarded as the internal forces and internal moments at the boundaries of the shell, with ν_α as the components of the unit normal $\mathbf{v} = \nu_\alpha \mathbf{e}_\alpha^r$ of Γ . Introducing these results into (34), we get

$$\int_\Omega (\mathbf{n}_{\alpha,\alpha} + \bar{\mathbf{n}} - \dot{\hat{\lambda}}) d\Omega + \int_\Gamma (\bar{\mathbf{n}}^\Gamma - \mathbf{n}^\Gamma) d\Gamma = \mathbf{o} \quad \text{and}$$

$$\int_\Omega [\mathbf{z} \times (\mathbf{n}_{\alpha,\alpha} + \bar{\mathbf{n}} - \dot{\hat{\lambda}}) + (\mathbf{m}_{\alpha,\alpha} + \mathbf{z}_{,\alpha} \times \mathbf{n}_\alpha + \bar{\mathbf{m}} - \dot{\hat{\mu}})] d\Omega$$

$$+ \int_\Gamma [\mathbf{z} \times (\bar{\mathbf{n}}^\Gamma - \mathbf{n}^\Gamma) + (\bar{\mathbf{m}}^\Gamma - \mathbf{m}^\Gamma)] d\Gamma = \mathbf{o}, \tag{37}$$

from which it is possible to state

$$\left. \begin{array}{l} \mathbf{n}_{\alpha,\alpha} + \bar{\mathbf{n}} - \dot{\hat{\lambda}} = \mathbf{o} \quad \text{in } \Omega \\ \mathbf{n}^\Gamma = \bar{\mathbf{n}}^\Gamma \quad \text{on } \Gamma \\ \mathbf{m}_{\alpha,\alpha} + \mathbf{z}_{,\alpha} \times \mathbf{n}_\alpha + \bar{\mathbf{m}} - \dot{\hat{\mu}} = \mathbf{o} \quad \text{in } \Omega \\ \mathbf{m}^\Gamma = \bar{\mathbf{m}}^\Gamma \quad \text{on } \Gamma \end{array} \right\} \Rightarrow \begin{cases} \mathbf{f}^{\text{ext}} = \dot{\hat{\lambda}} \\ \mathbf{m}^{\text{ext}} = \dot{\hat{\mu}}. \end{cases} \tag{38}$$

The first and the third expressions above represent the local equations of motion for this shell model. The second and the fourth expressions constitute the natural boundary conditions.

3.7 Weak form of the equations of motion

One possible strong form for the local equations of motion (38) is

$$\int_\Omega (\mathbf{n}_{\alpha,\alpha} + \bar{\mathbf{n}} - \dot{\hat{\lambda}}) \cdot \delta \dot{\mathbf{u}} d\Omega + \int_\Gamma (\bar{\mathbf{n}}^\Gamma - \mathbf{n}^\Gamma) \cdot \delta \dot{\mathbf{u}} d\Gamma$$

$$+ \int_\Omega (\mathbf{m}_{\alpha,\alpha} + \mathbf{z}_{,\alpha} \times \mathbf{n}_\alpha + \bar{\mathbf{m}} - \dot{\hat{\mu}}) \cdot \delta \boldsymbol{\omega} d\Omega$$

$$+ \int_\Gamma (\bar{\mathbf{m}}^\Gamma - \mathbf{m}^\Gamma) \cdot \delta \boldsymbol{\omega} d\Gamma = 0, \quad \forall \delta \dot{\mathbf{u}}, \delta \boldsymbol{\omega}, \tag{39}$$

where $\delta \dot{\mathbf{u}}$ and $\delta \boldsymbol{\omega}$ are adopted as weighting functions. On the other hand, from the divergence theorem on the cross-sectional resultants \mathbf{n}_α and \mathbf{m}_α , it follows

$$\int_\Omega \mathbf{n}_{\alpha,\alpha} \cdot \delta \dot{\mathbf{u}} d\Omega = - \int_\Omega \mathbf{n}_\alpha \cdot \delta \dot{\mathbf{u}}_{,\alpha} d\Omega + \int_\Gamma (\mathbf{n}^\Gamma \cdot \delta \dot{\mathbf{u}}) d\Gamma \quad \text{and}$$

$$\int_\Omega \mathbf{m}_{\alpha,\alpha} \cdot \delta \boldsymbol{\omega} d\Omega = - \int_\Omega \mathbf{m}_\alpha \cdot \delta \boldsymbol{\omega}_{,\alpha} d\Omega + \int_\Gamma (\mathbf{m}^\Gamma \cdot \delta \boldsymbol{\omega}) d\Gamma, \tag{40}$$

with \mathbf{n}^Γ and \mathbf{m}^Γ as in (36). Introducing (40) into (39) leads to the following weak form, which corresponds to the Virtual Power Theorem:

$$\delta P = \int_\Omega [\mathbf{n}_\alpha \cdot (\delta \dot{\mathbf{u}}_{,\alpha} + \mathbf{z}_{,\alpha} \times \delta \boldsymbol{\omega}) + (\dot{\hat{\lambda}} - \bar{\mathbf{n}}) \cdot \delta \dot{\mathbf{u}}] d\Omega$$

$$- \int_\Gamma (\bar{\mathbf{n}}^\Gamma \cdot \delta \dot{\mathbf{u}}) d\Gamma$$

$$+ \int_\Omega [\mathbf{m}_\alpha \cdot \delta \boldsymbol{\omega}_{,\alpha} + (\dot{\hat{\mu}} - \bar{\mathbf{m}}) \cdot \delta \boldsymbol{\omega}] d\Omega$$

$$- \int_\Gamma (\bar{\mathbf{m}}^\Gamma \cdot \delta \boldsymbol{\omega}) d\Gamma = 0, \quad \forall \delta \dot{\mathbf{u}}, \delta \boldsymbol{\omega}. \tag{41}$$

Expression (41) may be written in a more compact manner as follows

$$\delta P = \int_\Omega (\boldsymbol{\sigma}_\alpha \cdot \boldsymbol{\Phi}_\alpha \boldsymbol{\Delta}_\alpha \delta \mathbf{v} + \dot{\hat{\mathbf{g}}} \cdot \delta \mathbf{v} - \bar{\boldsymbol{\sigma}} \cdot \delta \mathbf{v}) d\Omega$$

$$- \int_\Gamma (\bar{\boldsymbol{\sigma}}^\Gamma \cdot \delta \mathbf{v}) d\Gamma = 0, \quad \forall \delta \mathbf{v}, \tag{42}$$

where $\boldsymbol{\sigma}_\alpha$, $\boldsymbol{\Phi}_\alpha$ and $\boldsymbol{\Delta}_\alpha$ are given by expressions (26) and (20) and

$$\delta \mathbf{v} = \begin{bmatrix} \delta \dot{\mathbf{u}} \\ \delta \boldsymbol{\omega} \end{bmatrix}, \quad \dot{\hat{\mathbf{g}}} = \begin{bmatrix} \dot{\hat{\lambda}} \\ \dot{\hat{\mu}} \end{bmatrix}, \quad \bar{\boldsymbol{\sigma}} = \begin{bmatrix} \bar{\mathbf{n}} \\ \bar{\mathbf{m}} \end{bmatrix} \quad \text{and} \quad \bar{\boldsymbol{\sigma}}^\Gamma = \begin{bmatrix} \bar{\mathbf{n}}^\Gamma \\ \bar{\mathbf{m}}^\Gamma \end{bmatrix}. \tag{43}$$

As in [15] for rods, we remark that due to the use of $\delta \dot{\mathbf{u}}$ and $\delta \boldsymbol{\omega}$ as weighting functions the static part of Eq. (42) does not constitute the variation of a functional. For this reason, a symmetric tangent of the weak form is not to be expected. However, this does not represent a drawback, since the presence of rotational degrees-of-freedom leads anyway to a nonsymmetrical dynamical problem. Another possible weak form for the equations of motion may be constructed via the Virtual Work Theorem, but demonstration of energy conservation within the time integration scheme becomes extremely complicated—if not impossible. We adopt (42) as the basis in the development of our algorithm and associated finite element approximation.

3.8 Shell energy and constitutive equation

We assume that the shell is made of a hyperelastic material and is under a plane-stress state, with $\psi = \hat{\psi}(\mathbf{e}_1^r, \mathbf{e}_2^r)$ as its specific strain energy function per unit volume of the reference configuration. The shell internal energy is then written as

$$U^{\text{int}} = \int_{\Omega} \int_H \psi(\mathbf{e}_1^r, \mathbf{e}_2^r) dH d\Omega = \int_{\Omega} \bar{\psi}(\mathbf{e}_1^r, \mathbf{e}_2^r) d\Omega, \quad (44)$$

where

$$\bar{\psi}(\mathbf{e}_1^r, \mathbf{e}_2^r) = \int_H \psi(\mathbf{e}_1^r, \mathbf{e}_2^r) dH \quad (45)$$

may be regarded as the strain energy of the cross-sections. The kinetic energy, in its turn, reads as

$$T = \frac{1}{2} \int_{\Omega} \int_H \rho \dot{\mathbf{x}} \cdot \dot{\mathbf{x}} dH d\Omega = \frac{1}{2} \int_{\Omega} \bar{T} d\Omega, \quad \text{with}$$

$$\bar{T} = \frac{1}{2} \bar{M} \dot{\mathbf{u}} \cdot \dot{\mathbf{u}} + \frac{1}{2} \bar{\mathbf{J}} \boldsymbol{\omega} \cdot \boldsymbol{\omega} = \frac{1}{2} \bar{M} \dot{\mathbf{u}} \cdot \dot{\mathbf{u}} + \frac{1}{2} \bar{\mathbf{J}}^r \boldsymbol{\omega}^r \cdot \boldsymbol{\omega}^r. \quad (46)$$

The stress resultants σ_{α}^r and the matrices of material tangent moduli $\mathbf{D}_{\alpha\beta}^r$ may be derived from $\bar{\psi}$ as follows:

$$\sigma_{\alpha}^r = \frac{\partial \bar{\psi}}{\partial \mathbf{e}_{\alpha}^r} \quad \text{and} \quad \mathbf{D}_{\alpha\beta}^r = \frac{\partial \sigma_{\alpha}^r}{\partial \mathbf{e}_{\beta}^r} = \frac{\partial^2 \bar{\psi}}{\partial \mathbf{e}_{\alpha}^r \partial \mathbf{e}_{\beta}^r}. \quad (47)$$

Some possible choices for $\bar{\psi}$ (or, equivalently, for ψ) are discussed next.

Linear elastic material

A linear elastic material may be defined by setting a quadratic potential

$$\bar{\psi}(\mathbf{e}_1^r, \mathbf{e}_2^r) = \frac{1}{2} \mathbf{e}_{\alpha}^r \cdot \mathbf{D}_{\alpha\beta}^r \mathbf{e}_{\beta}^r, \quad (48)$$

taking $\mathbf{D}_{\alpha\beta}^r$ as constant so that from definition (47) follows

$$\sigma_{\alpha}^r = \mathbf{D}_{\alpha\beta}^r \mathbf{e}_{\beta}^r. \quad (49)$$

Recalling that we assume that the shell mid-surface is the medium surface, matrices $\mathbf{D}_{\alpha\beta}^r$ are given in the shell's local system by the standard relations

$$\mathbf{D}_{11}^r = \frac{\partial \sigma_1^r}{\partial \mathbf{e}_1^r} = \begin{bmatrix} \bar{E}h & 0 & 0 & 0 & 0 & 0 \\ 0 & \mu h & 0 & 0 & 0 & 0 \\ 0 & 0 & \mu h & 0 & 0 & 0 \\ 0 & 0 & 0 & \frac{1}{12} \mu h^3 & 0 & 0 \\ 0 & 0 & 0 & 0 & \frac{1}{12} \bar{E}h^3 & 0 \\ 0 & 0 & 0 & 0 & 0 & 0 \end{bmatrix}, \quad (50)$$

$$\mathbf{D}_{12}^r = \frac{\partial \sigma_1^r}{\partial \mathbf{e}_2^r} = \begin{bmatrix} 0 & \bar{E}vh & 0 & 0 & 0 & 0 \\ \mu h & 0 & 0 & 0 & 0 & 0 \\ 0 & 0 & 0 & 0 & 0 & 0 \\ 0 & 0 & 0 & 0 & -\frac{1}{12} \mu h^3 & 0 \\ 0 & 0 & 0 & -\frac{1}{12} \bar{E}vh^3 & 0 & 0 \\ 0 & 0 & 0 & 0 & 0 & 0 \end{bmatrix}$$

$$= \mathbf{D}_{21}^{rT}, \quad \text{and} \quad (51)$$

$$\mathbf{D}_{22}^r = \frac{\partial \sigma_2^r}{\partial \mathbf{e}_2^r} = \begin{bmatrix} \mu h & 0 & 0 & 0 & 0 & 0 \\ 0 & \bar{E}h & 0 & 0 & 0 & 0 \\ 0 & 0 & \mu h & 0 & 0 & 0 \\ 0 & 0 & 0 & \frac{1}{12} \bar{E}h^3 & 0 & 0 \\ 0 & 0 & 0 & 0 & \frac{1}{12} \mu h^3 & 0 \\ 0 & 0 & 0 & 0 & 0 & 0 \end{bmatrix}, \quad (52)$$

in which \bar{E} is the effective elasticity modulus, μ is the transverse shear modulus and ν the Poisson's coefficient. One should remind that $\bar{E} = E/(1 - \nu^2)$ and $\mu = E/2(1 + \nu)$, with E as the standard elasticity modulus. Small strains must be assumed for this constitutive relation to be valid.

Neo-Hookean elastic material

If we assume that the material is isotropic, the specific strain energy function $\psi(\mathbf{e}_1^r, \mathbf{e}_2^r)$ may be rewritten in terms of strain invariants I_1 and I_2 . By adopting $I_1 = \mathbf{F} : \mathbf{F}$ and $I_2 = \det \mathbf{F} = J$, a neo-Hookean hyperelastic material may be defined by (see e.g. [8])

$$\psi(I_1, J) = \frac{1}{2} \lambda \left[\frac{1}{2} (J^2 - 1) - \ln J \right] + \frac{1}{2} \mu (I_1 - 3 - 2 \ln J), \quad (53)$$

where λ and μ are elastic parameters or generalized Lamé constants.

In order to enforce the plane-stress condition in a consistent manner, let us rewrite expression (15) for the deformation gradient as

$$\mathbf{F} = \mathbf{Q}[\mathbf{I} + (\boldsymbol{\eta}_{\alpha}^r + \boldsymbol{\kappa}_{\alpha}^r \times \mathbf{r}^r) \otimes \mathbf{e}_{\alpha}^r + \gamma_{33} \mathbf{e}_3^r \otimes \mathbf{e}_3^r] = \mathbf{Q}[\mathbf{I} + \boldsymbol{\gamma}_{\alpha}^r \otimes \mathbf{e}_{\alpha}^r + \boldsymbol{\gamma}_3^r \otimes \mathbf{e}_3^r], \quad (54)$$

in which $\boldsymbol{\gamma}_{\alpha}^r = \boldsymbol{\eta}_{\alpha}^r + \boldsymbol{\kappa}_{\alpha}^r \times \mathbf{r}^r$ enclose the shell strain vectors and $\boldsymbol{\gamma}_3^r = \gamma_{33} \mathbf{e}_3^r$ is the vector of thickness straining

corresponding to the plane-stress state (scalar γ_{33} is here introduced to allow for this thickness deformation). Defining

$$\mathbf{f}_i^r = \mathbf{e}_i^r + \boldsymbol{\gamma}_i^r, \tag{55}$$

expression (54) can be further rewritten as

$$\mathbf{F} = \mathbf{Q}(\mathbf{f}_i^r \otimes \mathbf{e}_i^r), \tag{56}$$

and in this case the strain invariants turn out to be

$$\begin{aligned} I_1 &= \mathbf{f}_i^r \cdot \mathbf{f}_i^r = \mathbf{f}_\alpha^r \cdot \mathbf{f}_\alpha^r + (1 + \gamma_{33})^2 \quad \text{and} \\ J &= \mathbf{f}_3^r \cdot (\mathbf{f}_1^r \times \mathbf{f}_2^r) = (1 + \gamma_{33})\bar{J}, \quad \text{with} \\ \bar{J} &= \mathbf{e}_3^r \cdot (\mathbf{f}_1^r \times \mathbf{f}_2^r). \end{aligned} \tag{57}$$

It is not difficult to show that the derivatives of $\psi(I_1, J)$ with respect to \mathbf{f}_i^r furnish the first Piola–Kirchhoff stresses $\boldsymbol{\tau}_i^r$ as below

$$\boldsymbol{\tau}_i^r = \frac{\partial \psi}{\partial \mathbf{f}_i^r} = \frac{\partial \psi}{\partial I_1} \frac{\partial I_1}{\partial \mathbf{f}_i^r} + \frac{\partial \psi}{\partial J} \frac{\partial J}{\partial \mathbf{f}_i^r}, \tag{58}$$

and after some algebra one has

$$\begin{aligned} \boldsymbol{\tau}_\alpha^r &= 2 \frac{\partial \psi}{\partial I_1} \mathbf{f}_\alpha^r + \frac{\partial \psi}{\partial J} (1 + \gamma_{33}) (\varepsilon_{\alpha\beta\gamma} \mathbf{f}_\beta^r \times \mathbf{e}_\gamma^r) \quad \text{and} \\ \tau_{33} &= \boldsymbol{\tau}_3^r \cdot \mathbf{e}_3^r = 2(1 + \gamma_{33}) \frac{\partial \psi}{\partial I_1} + \frac{\partial \psi}{\partial J} \bar{J}, \end{aligned} \tag{59}$$

with $\varepsilon_{\alpha\beta\gamma} = \mathbf{e}_\alpha^r \cdot \mathbf{e}_\beta^r \times \mathbf{e}_\gamma^r$ as a permutation symbol. Now the plane-stress assumption

$$\tau_{33} = \boldsymbol{\tau}_3^r \cdot \mathbf{e}_3^r = 0 \tag{60}$$

may be invoked for Eq. (59)₂, and with the aid of (53) it renders

$$\gamma_{33} = \sqrt{\frac{\lambda + 2\mu}{\lambda \bar{J}^2 + 2\mu}} - 1, \tag{61}$$

i.e. γ_{33} may be eliminated. Introducing this result into (59)₁, and taking (53) again into account, the following expression is obtained for the first Piola–Kirchhoff stress vectors:

$$\boldsymbol{\tau}_\alpha^r = \varphi(\bar{J}) \varepsilon_{\alpha\beta\gamma} \mathbf{f}_\beta^r \times \mathbf{e}_\gamma^r + \mu \mathbf{f}_\alpha^r, \tag{62}$$

where

$$\varphi(\bar{J}) = \left[\frac{1}{2} \lambda (J^2 - 1) - \mu \right] \frac{1}{\bar{J}} = -\mu \frac{\lambda + 2\mu}{\lambda \bar{J}^3 + 2\mu \bar{J}}. \tag{63}$$

The stress resultants $\boldsymbol{\sigma}_\alpha^r$ may be then computed via integration of (62) across the thickness. Alternatively, one may use expression (47)₁ together with (45), (57) and (61) to get $\boldsymbol{\sigma}_\alpha^r$.

For computation of the matrices of material tangent moduli, from (47)₂ one has

$$\mathbf{D}_{\alpha\beta}^r = \frac{\partial \boldsymbol{\sigma}_\alpha^r}{\partial \mathbf{e}_\beta^r} = \begin{bmatrix} \frac{\partial \mathbf{n}_\alpha^r}{\partial \boldsymbol{\eta}_\beta^r} & \frac{\partial \mathbf{n}_\alpha^r}{\partial \boldsymbol{\kappa}_\beta^r} \\ \frac{\partial \mathbf{m}_\alpha^r}{\partial \boldsymbol{\eta}_\beta^r} & \frac{\partial \mathbf{m}_\alpha^r}{\partial \boldsymbol{\kappa}_\beta^r} \end{bmatrix}. \tag{64}$$

Defining the tangent tensors

$$\mathbf{C}_{\alpha\beta}^r = \frac{\partial \boldsymbol{\tau}_\alpha^r}{\partial \boldsymbol{\gamma}_\beta^r}, \tag{65}$$

the derivatives in (64) may be written as

$$\begin{aligned} \frac{\partial \mathbf{n}_\alpha^r}{\partial \boldsymbol{\eta}_\beta^r} &= \int_H \mathbf{C}_{\alpha\beta}^r dH, \quad \frac{\partial \mathbf{n}_\alpha^r}{\partial \boldsymbol{\kappa}_\beta^r} = - \int_H \mathbf{C}_{\alpha\beta}^r \mathbf{R}^r dH, \\ \frac{\partial \mathbf{m}_\alpha^r}{\partial \boldsymbol{\eta}_\beta^r} &= \int_H \mathbf{R}^r \mathbf{C}_{\alpha\beta}^r dH \quad \text{and} \quad \frac{\partial \mathbf{m}_\alpha^r}{\partial \boldsymbol{\kappa}_\beta^r} = - \int_H \mathbf{R}^r \mathbf{C}_{\alpha\beta}^r \mathbf{R}^r dH, \end{aligned} \tag{66}$$

with $\mathbf{R}^r = \text{Skew}(\mathbf{r}^r)$. Substitution of (62) into (65) yields $\mathbf{C}_{\alpha\beta}^r$ as follows

$$\begin{aligned} \mathbf{C}_{\alpha\beta}^r &= \varphi'(\bar{J}) (\varepsilon_{\alpha\beta\gamma} \mathbf{f}_\gamma^r \times \mathbf{e}_\delta^r) \otimes (\varepsilon_{\beta\delta\gamma} \mathbf{f}_\gamma^r \times \mathbf{e}_\delta^r) \\ &\quad - \varphi(\bar{J}) \varepsilon_{\alpha\beta\gamma} \text{Skew}(\mathbf{e}_\gamma^r) + \mu \delta_{\alpha\beta} \mathbf{I}, \end{aligned} \tag{67}$$

where $\delta_{\alpha\beta}$ is the Kronecker symbol and

$$\begin{aligned} \varphi'(\bar{J}) &= \frac{\partial \varphi}{\partial \bar{J}} = \mu \frac{(\lambda + 2\mu)(3\lambda \bar{J}^2 + 2\mu)}{(\lambda \bar{J}^3 + 2\mu \bar{J})^2} \\ &= -\varphi(\bar{J}) \frac{3\lambda \bar{J}^2 + 2\mu}{\lambda \bar{J}^3 + 2\mu \bar{J}}. \end{aligned} \tag{68}$$

Substitution of (66) and (67) into (64) furnishes the matrices of material tangent moduli $\mathbf{D}_{\alpha\beta}^r$ for this neo-Hookean material. It is interesting to observe that, up to first order in the deformations, this material is entirely equivalent to the linear elastic material, as the above expressions for $\boldsymbol{\sigma}_\alpha^r$ and $\mathbf{D}_{\alpha\beta}^r$ collapse to the corresponding ones from the previous item.

Remark Fully three-dimensional hyperelastic materials (i.e. without the plane-stress enforcement) can be considered in the lines of [13]. Nevertheless, additional degrees-of-freedom pertaining to the cross-sections are necessary in order to account for the thickness straining.

4 Time increment

In this section we recast for the case of shells our time-increment notation introduced in [15] for rods. Additionally, some crucial results needed within the scheme are derived. We recall that an updated description will be applied, and for this reason the concepts of incremental displacements and incremental rotations will be fully exploited.

Consider an arbitrary time increment (t_i, t_{i+1}) , for which we adopt the notation $(\cdot)(t_i) = (\cdot)_i$ and $(\cdot)(t_{i+1}) = (\cdot)_{i+1}$. Assume that all quantities at time t_i are known from the solution at the previous increment and consider the following notation

$$\Delta(\cdot) = (\cdot)_{i+1} - (\cdot)_i \quad \text{and} \quad (\cdot)_{1/2} = \frac{1}{2} [(\cdot)_i + (\cdot)_{i+1}]. \tag{69}$$

Properties

$$(\cdot)_{1/2} + \frac{1}{2}\Delta(\cdot) = (\cdot)_{i+1} \quad \text{and} \quad (\cdot)_{1/2} - \frac{1}{2}\Delta(\cdot) = (\cdot)_i \quad (70)$$

hold and will be useful later on. If $*$ is a generic product and A and B are generic quantities, then one can show the following general result

$$\Delta(A * B) = A_{1/2} * \Delta B + \Delta A * B_{1/2}. \quad (71)$$

4.1 Incremental displacements and rotations

Let \mathbf{u}_Δ and \mathbf{Q}_Δ be the incremental displacement vector and the incremental rotation tensor, respectively, defined such that

$$\mathbf{u}_\Delta = \Delta \mathbf{u} \quad \text{and} \quad \mathbf{Q}_{i+1} = \mathbf{Q}_\Delta \mathbf{Q}_i. \quad (72)$$

Let α_Δ be the Rodrigues rotation vector associated to the rotation tensor \mathbf{Q}_Δ , with magnitude $\alpha_\Delta = \|\alpha_\Delta\|$, and let us write

$$\mathbf{A}_\Delta = \text{Skew}(\alpha_\Delta). \quad (73)$$

If \mathbf{u}_Δ and α_Δ are known, update of the displacement field may be performed by means of (72) and (69)₁, i.e

$$\mathbf{u}_{i+1} = \mathbf{u}_i + \mathbf{u}_\Delta, \quad (74)$$

and update of the rotation field may be performed by using the Rodrigues expression for superposed rotations (see [1, 17]):

$$\alpha_{i+1} = \frac{4}{4 - \alpha_\Delta \cdot \alpha_i} \left(\alpha_\Delta + \alpha_i + \frac{1}{2} \alpha_\Delta \times \alpha_i \right). \quad (75)$$

As previously stated in Part 1 of this work, we remark that expression (75) is valid only when the Rodrigues parameterization is adopted for the rotation field. For any other type of parameterization, update is a much more complicated task and requires many additional operations, sometimes with several singularities involved.

Let us now define the back-rotated incremental rotation tensor by

$$\mathbf{Q}_\Delta^r = \mathbf{Q}_{i+1}^T \mathbf{Q}_\Delta \mathbf{Q}_{i+1} = \mathbf{Q}_i^T \mathbf{Q}_\Delta \mathbf{Q}_i, \quad (76)$$

with α_Δ^r as its Rodrigues rotation vector, and let us write $\mathbf{A}_\Delta^r = \text{Skew}(\alpha_\Delta^r)$. From (76) and (72)₂, it follows

$$\alpha_\Delta^r = \mathbf{Q}_{i+1}^T \alpha_\Delta = \mathbf{Q}_i^T \alpha_\Delta \quad \text{and} \quad \alpha_\Delta = \|\alpha_\Delta^r\| = \|\alpha_\Delta\|. \quad (77)$$

Using (4) and (5), the following identities can be derived

$$\begin{aligned} \mathbf{Q}_{1/2} &= \frac{1}{2} \mathbf{Q}_i (\mathbf{I} + \mathbf{Q}_\Delta^r) = \mathbf{Q}_i \left(\mathbf{I} - \frac{1}{2} \mathbf{A}_\Delta^r \right)^{-1} \\ &= \mathbf{Q}_{i+1} \left(\mathbf{I} + \frac{1}{2} \mathbf{A}_\Delta^r \right)^{-1} \\ &= \frac{1}{2} (\mathbf{I} + \mathbf{Q}_\Delta) \mathbf{Q}_i = \left(\mathbf{I} - \frac{1}{2} \mathbf{A}_\Delta \right)^{-1} \mathbf{Q}_i \\ &= \left(\mathbf{I} + \frac{1}{2} \mathbf{A}_\Delta \right)^{-1} \mathbf{Q}_{i+1} \quad \text{and} \\ \Delta \mathbf{Q} &= \mathbf{Q}_{i+1} - \mathbf{Q}_i = \mathbf{Q}_i (\mathbf{Q}_\Delta^r - \mathbf{I}) \\ &= \mathbf{Q}_i \left(\mathbf{I} - \frac{1}{2} \mathbf{A}_\Delta^r \right)^{-1} \mathbf{A}_\Delta^r = \mathbf{Q}_{1/2} \mathbf{A}_\Delta^r \\ &= \mathbf{Q}_i \mathbf{A}_\Delta^r \left(\mathbf{I} - \frac{1}{2} \mathbf{A}_\Delta^r \right)^{-1} = \mathbf{Q}_i \mathbf{A}_\Delta^r \mathbf{Q}_i^T \mathbf{Q}_i \left(\mathbf{I} - \frac{1}{2} \mathbf{A}_\Delta^r \right)^{-1} \\ &= \mathbf{A}_\Delta \mathbf{Q}_{1/2}, \end{aligned} \quad (78)$$

and here one should notice that tensor $\mathbf{Q}_{1/2}$ is not a rotation tensor, but verifies both equations $\alpha_\Delta^r = \mathbf{Q}_{1/2}^T \alpha_\Delta$ and $\alpha_\Delta = \mathbf{Q}_{1/2} \alpha_\Delta^r$. These relations can be obtained with the aid of (77)₁. Other important expressions involving $\mathbf{Q}_{1/2}$ may be derived by using (9):

$$\begin{aligned} \det(\mathbf{Q}_{1/2}) &= h(\alpha_\Delta), \quad \mathbf{Q}_{1/2} = \det(\mathbf{Q}_{1/2}) \boldsymbol{\Xi}_\Delta^{-T} \mathbf{Q}_i, \\ \mathbf{Q}_{1/2}^{-1} &= \det(\mathbf{Q}_{1/2})^{-1} \mathbf{Q}_i^T \boldsymbol{\Xi}_\Delta^T \quad \text{and} \quad \det(\mathbf{Q}_{1/2}) \mathbf{Q}_{1/2}^{-T} = \boldsymbol{\Xi}_\Delta \mathbf{Q}_i, \end{aligned} \quad (79)$$

where

$$\boldsymbol{\Xi}_\Delta = \hat{\boldsymbol{\Xi}}(\alpha_\Delta) = h(\alpha_\Delta) \left(\mathbf{I} + \frac{1}{2} \mathbf{A}_\Delta \right). \quad (80)$$

The following Nanson’s rule may also be written:

$$\begin{aligned} (\mathbf{Q}_{1/2} \mathbf{a}) \times (\mathbf{Q}_{1/2} \mathbf{b}) &= \det(\mathbf{Q}_{1/2}) \mathbf{Q}_{1/2}^{-T} (\mathbf{a} \times \mathbf{b}) \\ &= \boldsymbol{\Xi}_\Delta \mathbf{Q}_i (\mathbf{a} \times \mathbf{b}), \quad \forall \mathbf{a}, \mathbf{b} \in \mathbb{R}^3. \end{aligned} \quad (81)$$

4.2 Incremental strains

Starting from expression (16) for η_α^r and κ_α^r , and using (71), (72)₂ and (78), one can readily show that

$$\begin{aligned} \Delta \eta_\alpha^r &= \Delta(\mathbf{Q}^T \mathbf{z}_{,\alpha} - \mathbf{e}_\alpha^r) \\ &= \mathbf{Q}_{1/2}^T \mathbf{u}_{\Delta,\alpha} - \mathbf{Q}_{1/2}^T \mathbf{A}_\Delta \mathbf{z}_{1/2,\alpha} \\ &= \mathbf{Q}_{1/2}^T (\mathbf{u}_{\Delta,\alpha} + \mathbf{z}_{1/2,\alpha} \times \alpha_\Delta) \end{aligned} \quad (82)$$

and

$$\begin{aligned} \Delta \kappa_\alpha^r &= \kappa_{\alpha i+1}^r - \kappa_{\alpha i}^r \\ &= \mathbf{Q}_{i+1}^T \text{axial}(\mathbf{Q}_{i+1,\alpha} \mathbf{Q}_{i+1}^T) - \kappa_{\alpha i}^r = \mathbf{Q}_i^T \boldsymbol{\Xi}_\Delta^T \alpha_{\Delta,\alpha} \\ &= \det(\mathbf{Q}_{1/2}) \mathbf{Q}_{1/2}^{-1} \alpha_{\Delta,\alpha}. \end{aligned} \quad (83)$$

With these expressions, the incremental strain vectors $\Delta \boldsymbol{\varepsilon}_\alpha^r$ may be written in a compact manner as

$$\Delta \boldsymbol{\varepsilon}_\alpha^r = \mathbf{A}_m^T \boldsymbol{\Phi}_{\alpha 1/2} \boldsymbol{\Delta}_\alpha \mathbf{d}_\Delta, \tag{84}$$

in which

$$\begin{aligned} \mathbf{A}_m &= \begin{bmatrix} \mathbf{Q}_{1/2} & \mathbf{O} \\ \mathbf{O} & \det(\mathbf{Q}_{1/2}) \mathbf{Q}_{1/2}^{-T} \end{bmatrix}, \\ \boldsymbol{\Phi}_{\alpha 1/2} &= \begin{bmatrix} \mathbf{I} & \mathbf{O} & \mathbf{Z}_{1/2, \alpha} \\ \mathbf{O} & \mathbf{I} & \mathbf{O} \end{bmatrix} \\ \text{and } \mathbf{d}_\Delta &= \begin{bmatrix} \mathbf{u}_\Delta \\ \boldsymbol{\alpha}_\Delta \end{bmatrix}. \end{aligned} \tag{85}$$

Consistent linearization of (82) and (83) leads to

$$\begin{aligned} \delta \Delta \boldsymbol{\eta}_\alpha^r &= \delta \boldsymbol{\eta}_{\alpha i+1}^r = \mathbf{Q}_{i+1}^T [\delta \mathbf{u}_{\Delta, \alpha} + \mathbf{Z}_{i+1, \alpha} \boldsymbol{\Xi}_\Delta \delta \boldsymbol{\alpha}_\Delta] \text{ and} \\ \delta \Delta \boldsymbol{\kappa}_\alpha^r &= \delta \boldsymbol{\kappa}_{\alpha i+1}^r = \mathbf{Q}_i^T [\boldsymbol{\Xi}_\Delta^T \delta \boldsymbol{\alpha}_{\Delta, \alpha} + \mathbf{W}(\boldsymbol{\alpha}_\Delta, \boldsymbol{\alpha}_{\Delta, \alpha}) \delta \boldsymbol{\alpha}_\Delta] \\ &= \mathbf{Q}_{i+1}^T [\boldsymbol{\Xi}_\Delta \delta \boldsymbol{\alpha}_{\Delta, \alpha} + \mathbf{Q}_\Delta \mathbf{W}(\boldsymbol{\alpha}_\Delta, \boldsymbol{\alpha}_{\Delta, \alpha}) \delta \boldsymbol{\alpha}_\Delta], \end{aligned} \tag{86}$$

so that

$$\begin{aligned} \delta \Delta \boldsymbol{\varepsilon}_\alpha^r &= \delta \boldsymbol{\varepsilon}_{\alpha i+1}^r = \mathbf{A}_{i+1}^T \boldsymbol{\Phi}_{\alpha i+1} \mathbf{Y}_{\alpha \Delta} \boldsymbol{\Delta}_\alpha \delta \mathbf{d}_\Delta, \text{ with} \\ \mathbf{Y}_{\alpha \Delta} &= \begin{bmatrix} \mathbf{I} & \mathbf{O} & \mathbf{O} \\ \mathbf{O} & \boldsymbol{\Xi}_\Delta & \mathbf{Q}_\Delta \mathbf{W}(\boldsymbol{\alpha}_\Delta, \boldsymbol{\alpha}_{\Delta, \alpha}) \\ \mathbf{O} & \mathbf{O} & \boldsymbol{\Xi}_\Delta \end{bmatrix}. \end{aligned} \tag{87}$$

Expression (87) will be useful for the derivation of the tangent of the weak form in Sect. 5.5. It can be regarded as the time-discrete version of (22).

4.3 Increments of momentum, kinetic and strain energy

From expressions (30) and (31), and after some algebraic manipulations in the same lines as in Part 1 of this work, increments of linear and angular momentum may be written as

$$\begin{aligned} \Delta \boldsymbol{\lambda} &= \int_\Omega \Delta \bar{\boldsymbol{\lambda}} \, d\Omega \text{ and} \\ \Delta \boldsymbol{\mu} &= \int_\Omega (\mathbf{z}_{1/2} \times \bar{\mathbf{M}} \Delta \dot{\mathbf{u}} + \mathbf{u}_\Delta \times \bar{\mathbf{M}} \dot{\mathbf{u}}_{1/2} + \Delta \bar{\boldsymbol{\mu}}) \, d\Omega, \end{aligned} \tag{88}$$

where

$$\begin{aligned} \Delta \bar{\boldsymbol{\lambda}} &= \bar{\mathbf{M}} \dot{\mathbf{u}}_\Delta \text{ and} \\ \Delta \bar{\boldsymbol{\mu}} &= \Delta(\mathbf{Q} \bar{\boldsymbol{\mu}}^r) = \mathbf{Q}_{1/2} \Delta \bar{\boldsymbol{\mu}}^r + \Delta \mathbf{Q} \bar{\boldsymbol{\mu}}_{1/2}^r \\ &= \mathbf{Q}_{1/2} (\Delta \bar{\boldsymbol{\mu}}^r + \mathbf{A}_\Delta^r \bar{\boldsymbol{\mu}}_{1/2}^r) \\ &= \mathbf{Q}_{1/2} [\bar{\mathbf{J}}^r \Delta \boldsymbol{\omega}^r + \boldsymbol{\alpha}_\Delta^r \times (\bar{\mathbf{J}}^r \boldsymbol{\omega}_{1/2}^r)]. \end{aligned} \tag{89}$$

From (89)₂, one derives

$$\Delta \bar{\boldsymbol{\mu}}^r = \bar{\mathbf{J}}^r \Delta \boldsymbol{\omega}^r = \mathbf{Q}_{1/2}^{-1} \Delta \bar{\boldsymbol{\mu}} - \boldsymbol{\alpha}_\Delta^r \times (\bar{\mathbf{J}}^r \boldsymbol{\omega}_{1/2}^r), \tag{90}$$

which, with the aid of (79), yields

$$\begin{aligned} \Delta \bar{\boldsymbol{\mu}}^r \cdot \boldsymbol{\alpha}_\Delta^r &= \mathbf{Q}_{1/2}^{-1} \Delta \bar{\boldsymbol{\mu}} \cdot \boldsymbol{\alpha}_\Delta^r = \mathbf{Q}_{1/2}^{-1} \Delta \bar{\boldsymbol{\mu}} \cdot \mathbf{Q}_{1/2}^T \boldsymbol{\alpha}_\Delta \\ &= \Delta \bar{\boldsymbol{\mu}} \cdot \boldsymbol{\alpha}_\Delta. \end{aligned} \tag{91}$$

Increments of kinetic and strain energy, on its turn, are computed by using (46) and (44) respectively:

$$\begin{aligned} \Delta T &= \int_\Omega \Delta \bar{T} \, d\Omega, \text{ where } \Delta \bar{T} = \Delta \bar{\boldsymbol{\lambda}} \cdot \dot{\mathbf{u}}_{1/2} + \Delta \bar{\boldsymbol{\mu}}^r \cdot \boldsymbol{\omega}_{1/2}^r, \\ \text{and } \Delta U^{\text{int}} &= \int_\Omega \Delta \bar{\psi} \, d\Omega. \end{aligned} \tag{92}$$

5 Time integration algorithm

5.1 Time collocation of the equations of motion

First, we write the global equations of motion (33) at some time instant t_m in the midst of the increment:

$$\mathbf{f}_m^{\text{ext}} = \int_\Omega \dot{\bar{\boldsymbol{\lambda}}}_m \, d\Omega \text{ and } \mathbf{m}_m^{\text{ext}} = \int_\Omega (\mathbf{z}_{1/2} \times \dot{\bar{\boldsymbol{\lambda}}}_m + \dot{\bar{\boldsymbol{\mu}}}_m) \, d\Omega. \tag{93}$$

Then, we assume from (27) that

$$\begin{aligned} \mathbf{f}_m^{\text{ext}} &= \int_\Omega \bar{\mathbf{n}}_m \, d\Omega + \int_\Gamma \bar{\mathbf{n}}_m^\Gamma \, d\Gamma \text{ and} \\ \mathbf{m}_m^{\text{ext}} &= \int_\Omega (\mathbf{z}_{1/2} \times \bar{\mathbf{n}}_m + \bar{\mathbf{m}}_m) \, d\Omega \\ &\quad + \int_\Gamma (\mathbf{z}_{1/2} \times \bar{\mathbf{n}}_m^\Gamma + \bar{\mathbf{m}}_m^\Gamma) \, d\Gamma, \end{aligned} \tag{94}$$

where $\bar{\mathbf{n}}_m$, $\bar{\mathbf{m}}_m$, $\bar{\mathbf{n}}_m^\Gamma$ and $\bar{\mathbf{m}}_m^\Gamma$ are mean values of the external loads within the time step that will be defined later. We also assume [starting from (32)] that

$$\begin{aligned} \dot{\bar{\boldsymbol{\lambda}}}_m &= \bar{\mathbf{M}} \dot{\mathbf{u}}_{1/2} \text{ and} \\ \dot{\bar{\boldsymbol{\mu}}}_m &= \mathbf{Q}_{1/2} \dot{\bar{\boldsymbol{\mu}}}_m^r, \text{ with } \dot{\bar{\boldsymbol{\mu}}}_m^r = \bar{\mathbf{J}}^r \dot{\boldsymbol{\omega}}_{1/2}^r + \boldsymbol{\omega}_{1/2}^r \times \bar{\mathbf{J}}^r \boldsymbol{\omega}_{1/2}^r, \end{aligned} \tag{95}$$

so that, by a similar ansatz as in (41), the weak form associated with (93) is given by

$$\begin{aligned} \delta P_m = & \int_{\Omega} [\mathbf{n}_{\alpha m} \cdot (\delta \dot{\mathbf{u}}_{,\alpha} + \mathbf{z}_{1/2,\alpha} \times \delta \boldsymbol{\omega}) + (\dot{\boldsymbol{\lambda}}_m - \bar{\mathbf{n}}_m) \cdot \delta \dot{\mathbf{u}}] d\Omega \\ & - \int_{\Gamma} (\bar{\mathbf{n}}_m^{\Gamma} \cdot \delta \dot{\mathbf{u}}) d\Gamma \\ & + \int_{\Omega} [\mathbf{m}_{\alpha m} \cdot \delta \boldsymbol{\omega}_{,\alpha} + (\dot{\boldsymbol{\mu}}_m - \bar{\mathbf{m}}_m) \cdot \delta \boldsymbol{\omega}] d\Omega \\ & - \int_{\Gamma} (\bar{\mathbf{m}}_m^{\Gamma} \cdot \delta \boldsymbol{\omega}) d\Gamma = 0. \end{aligned} \tag{96}$$

Here, $\mathbf{n}_{\alpha m}$ and $\mathbf{m}_{\alpha m}$ are mean values of the cross-sectional resultants within the time step, which will also be defined later. We can rewrite (96) as

$$\begin{aligned} \delta P_m = & \int_{\Omega} (\boldsymbol{\sigma}_{\alpha m} \cdot \boldsymbol{\Phi}_{\alpha 1/2} \boldsymbol{\Delta}_{\alpha} \delta \mathbf{v} + \dot{\mathbf{g}}_m \cdot \delta \mathbf{v} - \bar{\boldsymbol{\sigma}}_m \cdot \delta \mathbf{v}) d\Omega \\ & - \int_{\Gamma} (\bar{\boldsymbol{\sigma}}_m^{\Gamma} \cdot \delta \mathbf{v}) d\Gamma = 0, \quad \forall \delta \mathbf{v}, \end{aligned} \tag{97}$$

where $\boldsymbol{\Phi}_{\alpha 1/2}$ is given in (85) and (similarly to (43))

$$\begin{aligned} \boldsymbol{\sigma}_{\alpha m} = & \begin{bmatrix} \mathbf{n}_{\alpha m} \\ \mathbf{m}_{\alpha m} \end{bmatrix}, \quad \bar{\boldsymbol{\sigma}}_m = \begin{bmatrix} \bar{\mathbf{n}}_m \\ \bar{\mathbf{m}}_m \end{bmatrix}, \quad \bar{\boldsymbol{\sigma}}_m^{\Gamma} = \begin{bmatrix} \bar{\mathbf{n}}_m^{\Gamma} \\ \bar{\mathbf{m}}_m^{\Gamma} \end{bmatrix} \\ \text{and } \dot{\mathbf{g}}_m = & \begin{bmatrix} \dot{\boldsymbol{\lambda}}_m \\ \dot{\boldsymbol{\mu}}_m \end{bmatrix}. \end{aligned} \tag{98}$$

Notice that from (97) the algorithmic equations of motion (93) follows, by using (94) and (95).

One crucial aspect in our algorithm is now introduced: we define the cross-sectional resultants $\boldsymbol{\sigma}_{\alpha m}$ of (97) by

$$\boldsymbol{\sigma}_{\alpha m} = \boldsymbol{\Lambda}_m \boldsymbol{\sigma}_{\alpha m}^r, \tag{99}$$

with $\boldsymbol{\Lambda}_m$ as in (85) and $\boldsymbol{\sigma}_{\alpha m}^r$ given by

$$\boldsymbol{\sigma}_{\alpha m}^r = \begin{bmatrix} \int_H \boldsymbol{\tau}_{\alpha m}^r dH \\ \int_H \mathbf{r}^r \times \boldsymbol{\tau}_{\alpha m}^r dH \end{bmatrix}, \tag{100}$$

which is based on definitions (26) and (25). Here, we may regard $\boldsymbol{\tau}_{\alpha m}^r$ as mean values of the back-rotated first Piola–Kirchhoff stress vectors within the time increment, whose expressions will be defined later. Additionally, note from (99), (85)₁, (79)₄ and (81) that

$$\begin{aligned} \boldsymbol{\sigma}_{\alpha m} = & \begin{bmatrix} \int_H (\boldsymbol{Q}_{1/2} \boldsymbol{\tau}_{\alpha m}^r) dH \\ \int_H [(\boldsymbol{Q}_{1/2} \mathbf{r}^r) \times (\boldsymbol{Q}_{1/2} \boldsymbol{\tau}_{\alpha m}^r)] dH \end{bmatrix} \\ = & \begin{bmatrix} \int_H \boldsymbol{\tau}_{\alpha m} dH \\ \int_H (\mathbf{r}_{1/2} \times \boldsymbol{\tau}_{\alpha m}) dH \end{bmatrix}, \end{aligned} \tag{101}$$

in which

$$\boldsymbol{\tau}_{\alpha m} = \boldsymbol{Q}_{1/2} \boldsymbol{\tau}_{\alpha m}^r. \tag{102}$$

The above expression is a remarkable consequence of our collocation scheme: even though tensor $\boldsymbol{Q}_{1/2}$ is not a rotation, it operates as a rotation tensor over the algorithmic stresses $\boldsymbol{\tau}_{\alpha m}^r$.

5.2 Time approximations and algorithmic weak form

We adopt the following mid-step approximations for the time-dependent variables:

$$\begin{aligned} \dot{\mathbf{u}}_{1/2} = & \frac{1}{\Delta t} \mathbf{u}_{\Delta}, \\ \ddot{\mathbf{u}}_{1/2} = & \frac{1}{\Delta t} \dot{\mathbf{u}}_{\Delta} = \frac{2}{\Delta t^2} (\mathbf{u}_{\Delta} - \Delta t \dot{\mathbf{u}}_i), \\ \boldsymbol{\omega}_{1/2}^r = & \frac{1}{\Delta t} \boldsymbol{\alpha}_{\Delta}^r, \\ \dot{\boldsymbol{\omega}}_{1/2}^r = & \frac{1}{\Delta t} \Delta \boldsymbol{\omega}^r = \frac{2}{\Delta t^2} (\boldsymbol{\alpha}_{\Delta}^r - \Delta t \boldsymbol{\omega}_i^r). \end{aligned} \tag{103}$$

Introduction of these assumptions into (95) yields

$$\begin{aligned} \dot{\boldsymbol{\lambda}}_m = & \frac{2}{\Delta t^2} \bar{M} (\mathbf{u}_{\Delta} - \Delta t \dot{\mathbf{u}}_i) \quad \text{and} \\ \dot{\boldsymbol{\mu}}_m = & \boldsymbol{Q}_{1/2} \dot{\boldsymbol{\mu}}_m^r, \quad \text{with} \\ \dot{\boldsymbol{\mu}}_m^r = & \frac{2}{\Delta t^2} \left[\bar{J}^r (\boldsymbol{\alpha}_{\Delta}^r - \Delta t \boldsymbol{\omega}_i^r) + \frac{1}{2} \boldsymbol{\alpha}_{\Delta}^r \times \bar{J}^r \boldsymbol{\alpha}_{\Delta}^r \right]. \end{aligned} \tag{104}$$

By introducing (104) into (97), and by taking (99) into account, one arrives at the algorithmic weak form

$$\begin{aligned} \delta P_m = & \int_{\Omega} [\boldsymbol{\sigma}_{\alpha m}^r \cdot (\boldsymbol{\Lambda}_m^T \boldsymbol{\Phi}_{\alpha 1/2} \boldsymbol{\Delta}_{\alpha} \delta \mathbf{v}) + (\dot{\mathbf{g}}_m - \bar{\boldsymbol{\sigma}}_m) \cdot \delta \mathbf{v}] d\Omega \\ & - \int_{\Gamma} (\bar{\boldsymbol{\sigma}}_m^{\Gamma} \cdot \delta \mathbf{v}) d\Gamma = 0, \quad \forall \delta \mathbf{v}, \end{aligned} \tag{105}$$

where

$$\dot{\mathbf{g}}_m = \frac{2}{\Delta t^2} \left[\bar{M} (\mathbf{u}_{\Delta} - \Delta t \dot{\mathbf{u}}_i) + \boldsymbol{Q}_{1/2} \left(\bar{J}^r (\boldsymbol{\alpha}_{\Delta}^r - \Delta t \boldsymbol{\omega}_i^r) + \frac{1}{2} \boldsymbol{\alpha}_{\Delta}^r \times \bar{J}^r \boldsymbol{\alpha}_{\Delta}^r \right) \right]. \tag{106}$$

Expression (105) is crucial for the demonstration of energy conservation, as we will see next. However, as previously observed, a symmetric tangent of the weak form is not to be expected.

5.3 Conservation of linear and angular momentum

By inserting the time approximations (103) into the expressions of momentum increments, i.e. into (89), one arrives at

$$\begin{aligned} \Delta \bar{\boldsymbol{\lambda}} = & \Delta t (\bar{M} \dot{\mathbf{u}}_{1/2}), \quad \text{and} \\ \Delta \bar{\boldsymbol{\mu}} = & \Delta t \boldsymbol{Q}_{1/2} [\bar{J}^r \dot{\boldsymbol{\omega}}_{1/2}^r + \boldsymbol{\omega}_{1/2}^r \times (\bar{J}^r \boldsymbol{\omega}_{1/2}^r)]. \end{aligned} \tag{107}$$

With the aid of (93) and (95), after some algebra it follows that

$$\begin{aligned} \mathbf{f}_m^{\text{ext}} &= \frac{1}{\Delta t} \int_{\Omega} \Delta \bar{\boldsymbol{\lambda}} d\Omega = \frac{1}{\Delta t} \Delta \boldsymbol{\lambda} \quad \text{and} \\ \mathbf{m}_m^{\text{ext}} &= \frac{1}{\Delta t} \int_{\Omega} \Delta(\mathbf{z} \times \bar{\boldsymbol{\lambda}} + \bar{\boldsymbol{\mu}}) d\Omega = \frac{1}{\Delta t} \Delta \boldsymbol{\mu}, \end{aligned} \tag{108}$$

which means that if the body is isolated (i.e. if $\mathbf{f}_m^{\text{ext}} = \mathbf{m}_m^{\text{ext}} = \mathbf{o}$) both momenta are exactly conserved. More detailed steps in the obtaining of (108) can be found in Part 1 of this work. Expression (108) can be regarded as the algorithmic form of the Euler laws of motion.

5.4 Conservation of energy

By introducing (103) into (92)₁, and by using (91), after some manipulations

$$\Delta \bar{T} = \frac{1}{\Delta t} (\Delta \bar{\boldsymbol{\lambda}} \cdot \mathbf{u}_{\Delta} + \Delta \bar{\boldsymbol{\mu}} \cdot \boldsymbol{\alpha}_{\Delta}) = \dot{\mathbf{g}}_m \cdot \mathbf{d}_{\Delta} \tag{109}$$

follows. On the other hand, for isolated bodies the weak form (105) turns out to be

$$\delta P_m = \int_{\Omega} [\boldsymbol{\sigma}_{\alpha m}^r \cdot (\mathbf{A}_m^T \boldsymbol{\Phi}_{\alpha 1/2} \boldsymbol{\Delta}_{\alpha} \delta \mathbf{v}) + \dot{\mathbf{g}}_m \cdot \delta \mathbf{v}] d\Omega = 0, \quad \forall \delta \mathbf{v}, \tag{110}$$

so that if $\delta \mathbf{v} = \mathbf{d}_{\Delta}$ is set, and if (84) and (109) are taken into account, one has

$$\int_{\Omega} [\boldsymbol{\sigma}_{\alpha m}^r \cdot \Delta \boldsymbol{\epsilon}_{\alpha}^r + \Delta \bar{T}] d\Omega = 0. \tag{111}$$

This way, if $\boldsymbol{\sigma}_{\alpha m}^r$ is such that

$$\Delta \bar{\psi} = \boldsymbol{\sigma}_{\alpha m}^r \cdot \Delta \boldsymbol{\epsilon}_{\alpha}^r, \tag{112}$$

with $\bar{\psi}$ as the cross-sectional specific strain energy defined in (45), then the increment of mechanical energy (from (111)) vanishes, i.e. the total energy is exactly conserved in a discrete sense. In order to fulfill condition (112), $\boldsymbol{\sigma}_{\alpha m}^r$ is here defined by setting

$$\boldsymbol{\sigma}_{\alpha m}^r = \hat{\boldsymbol{\sigma}}_{\alpha}^r(\boldsymbol{\epsilon}_{1m}^r, \boldsymbol{\epsilon}_{2m}^r) = \frac{\partial \bar{\psi}}{\partial \boldsymbol{\epsilon}_{\alpha}^r}(\boldsymbol{\epsilon}_{1m}^r, \boldsymbol{\epsilon}_{2m}^r), \tag{113}$$

where the collocation points $\boldsymbol{\epsilon}_{\alpha m}^r$ are given by a convex combination of $\boldsymbol{\epsilon}_{\alpha}^r$ within the increment:

$$\boldsymbol{\epsilon}_{\alpha m}^r = \boldsymbol{\epsilon}_{\alpha}^r \vartheta = (1 - \vartheta) \boldsymbol{\epsilon}_{\alpha i}^r + \vartheta \boldsymbol{\epsilon}_{\alpha i+1}^r = \boldsymbol{\epsilon}_{\alpha i}^r + \vartheta \Delta \boldsymbol{\epsilon}_{\alpha}^r, \tag{114}$$

with ϑ as a local scalar variable yet to be determined. As we have previously mentioned in [15], this idea is similar to that proposed for solids by Simo and coworkers in [20], although in a different framework. Simo, however, did not consider the coupling between ϑ and the deformations (see discussion

in reference [11]), leading to an incorrect tangent operator. For this reason, only material laws with quadratic potentials could be handled in his approach, since for $\vartheta = 1/2$ the strain coupling automatically disappears. Here, more general hyperelastic materials can be considered and ϑ is found by solving the energy conservation constraint equation

$$g(\vartheta) = \boldsymbol{\sigma}_{\alpha m}^r \cdot \Delta \boldsymbol{\epsilon}_{\alpha}^r - \Delta \bar{\psi} = 0 \tag{115}$$

by the Newton method as follows

$$\begin{aligned} \vartheta_{k+1} &= \vartheta_k - [g'(\vartheta_k)]^{-1} g(\vartheta_k), \quad k = 1, 2, \dots, \quad \vartheta_0 = \frac{1}{2}, \\ \text{where } g'(\vartheta) &= [\mathbf{D}_{\alpha\beta}^r(\boldsymbol{\epsilon}_{1\vartheta}^r, \boldsymbol{\epsilon}_{2\vartheta}^r) \Delta \boldsymbol{\epsilon}_{\beta}^r] \cdot \Delta \boldsymbol{\epsilon}_{\alpha}^r, \end{aligned} \tag{116}$$

with $\mathbf{D}_{\alpha\beta}^r$ as in (47)₂.

As a consequence of assumption (114) and constraint (115), computation of the tangent of the weak form becomes much more elaborated. If we regard Eq. (115) as driven by the strain vectors $\boldsymbol{\epsilon}_{\alpha i+1}^r$ only, the following useful result may be obtained:

$$\begin{aligned} \frac{\partial g}{\partial \boldsymbol{\epsilon}_{\alpha i+1}^r} + \frac{\partial g}{\partial \vartheta} \frac{\partial \vartheta}{\partial \boldsymbol{\epsilon}_{\alpha i+1}^r} &= \boldsymbol{\sigma}_{\alpha m}^r - \boldsymbol{\sigma}_{\alpha i+1}^r \\ + \vartheta \mathbf{D}_{\alpha\delta}^r(\boldsymbol{\epsilon}_{1\vartheta}^r, \boldsymbol{\epsilon}_{2\vartheta}^r) \Delta \boldsymbol{\epsilon}_{\delta}^r + g'(\vartheta) \frac{\partial \vartheta}{\partial \boldsymbol{\epsilon}_{\alpha i+1}^r} &= 0, \end{aligned} \tag{117}$$

from where

$$\frac{\partial \vartheta}{\partial \boldsymbol{\epsilon}_{\alpha i+1}^r} = \frac{1}{g'(\vartheta)} [\boldsymbol{\sigma}_{\alpha i+1}^r - \boldsymbol{\sigma}_{\alpha m}^r - \vartheta \mathbf{D}_{\alpha\delta}^r(\boldsymbol{\epsilon}_{1\vartheta}^r, \boldsymbol{\epsilon}_{2\vartheta}^r) \Delta \boldsymbol{\epsilon}_{\delta}^r]. \tag{118}$$

With this expression, one may write

$$\begin{aligned} \mathbf{D}_{\alpha\beta}^{\text{alg}} &= \frac{\partial \boldsymbol{\sigma}_{\alpha m}^r}{\partial \boldsymbol{\epsilon}_{\beta i+1}^r} = \frac{\partial \boldsymbol{\sigma}_{\alpha m}^r}{\partial \boldsymbol{\epsilon}_{\delta m}^r} \frac{\partial \boldsymbol{\epsilon}_{\delta m}^r}{\partial \boldsymbol{\epsilon}_{\beta i+1}^r} \\ &= \mathbf{D}_{\alpha\beta}^r(\boldsymbol{\epsilon}_{1\vartheta}^r, \boldsymbol{\epsilon}_{2\vartheta}^r) \left[\vartheta \mathbf{I} + \Delta \boldsymbol{\epsilon}_{\delta}^r \otimes \frac{\partial \vartheta}{\partial \Delta \boldsymbol{\epsilon}_{\beta i+1}^r} \right] \\ &= \vartheta \mathbf{D}_{\alpha\beta}^r(\boldsymbol{\epsilon}_{1\vartheta}^r, \boldsymbol{\epsilon}_{2\vartheta}^r) \\ &\quad + \frac{1}{g'(\vartheta)} \mathbf{D}_{\alpha\delta}^r(\boldsymbol{\epsilon}_{1\vartheta}^r, \boldsymbol{\epsilon}_{2\vartheta}^r) \Delta \boldsymbol{\epsilon}_{\delta}^r \\ &\quad \otimes [\boldsymbol{\sigma}_{\beta i+1}^r - \boldsymbol{\sigma}_{\beta m}^r - \vartheta \mathbf{D}_{\beta\gamma}^r(\boldsymbol{\epsilon}_{1\vartheta}^r, \boldsymbol{\epsilon}_{2\vartheta}^r) \Delta \boldsymbol{\epsilon}_{\gamma}^r]. \end{aligned} \tag{119}$$

Notice that, if $\bar{\psi}$ is quadratic, one deduces $\vartheta = 1/2$ as an analytical solution to (115), and then

$$\begin{aligned} \boldsymbol{\epsilon}_{\alpha m}^r &= \boldsymbol{\epsilon}_{\alpha 1/2}^r, \quad \boldsymbol{\sigma}_{\alpha m}^r = \boldsymbol{\sigma}_{\alpha 1/2}^r = \mathbf{D}_{\alpha\beta}^r(\boldsymbol{\epsilon}_{11/2}^r, \boldsymbol{\epsilon}_{21/2}^r) \boldsymbol{\epsilon}_{\beta 1/2}^r, \\ \Delta \bar{\psi} &= \boldsymbol{\sigma}_{\alpha 1/2}^r \cdot \Delta \boldsymbol{\epsilon}_{\alpha}^r \quad \text{and} \quad \mathbf{D}_{\alpha\beta}^{\text{alg}} = \frac{1}{2} \mathbf{D}_{\alpha\beta}^r. \end{aligned} \tag{120}$$

Remark As we have mentioned in [15], and based on [20], one can argue that definition (113) would allow only for first-order accuracy within a time-stepping scheme, and that second-order accuracy would be attained by setting

$$\boldsymbol{\sigma}_{\alpha m}^r = \frac{1}{2} [\hat{\boldsymbol{\sigma}}_{\alpha}^r(\boldsymbol{\epsilon}_{1\vartheta}^r, \boldsymbol{\epsilon}_{2\vartheta}^r) + \hat{\boldsymbol{\sigma}}_{\alpha}^r(\boldsymbol{\epsilon}_{11-\vartheta}^r, \boldsymbol{\epsilon}_{21-\vartheta}^r)], \tag{121}$$

with $\mathbf{e}_{\alpha\vartheta}^r$ as in (114) and $\mathbf{e}_{\alpha 1-\vartheta}^r = \vartheta \mathbf{e}_{\alpha i}^r + (1 - \vartheta)\mathbf{e}_{\alpha i+1}^r = \mathbf{e}_{\alpha i+1}^r - \vartheta \Delta \mathbf{e}_{\alpha}^r$. In this case, the solution of constraint Eq. (115) requires

$$g'(\vartheta) = \frac{1}{2} [\mathbf{D}_{\alpha\beta}^r(\mathbf{e}_{1\vartheta}^r, \mathbf{e}_{2\vartheta}^r) + \mathbf{D}_{\alpha\beta}^r(\mathbf{e}_{1 1-\vartheta}^r, \mathbf{e}_{2 1-\vartheta}^r)] \Delta \mathbf{e}_{\beta}^r \cdot \Delta \mathbf{e}_{\alpha}^r, \tag{122}$$

and a corresponding $\mathbf{D}_{\alpha\beta}^{\text{alg}}$ arises. Algorithmic definition (121) increases computational effort substantially since every function must be evaluated twice at each integration point. Once second-order accuracy is an asymptotic concept, whether this additional effort is compensated by increased accuracy for finite time steps remains a matter of future research.

5.5 Tangent of the weak form

The Gateaux derivative of the algorithmic weak form (105) furnishes, after some lengthy algebra, the tangent of the weak form as given below

$$\begin{aligned} \delta(\delta P_m) = & \int_{\Omega} \Delta_{\alpha} \delta \mathbf{v} \cdot (\Phi_{\alpha 1/2}^T \Lambda_m \mathbf{D}_{\alpha\beta}^{\text{alg}} \Lambda_{i+1}^T \Phi_{\beta i+1} Y_{\beta \Delta} \Delta_{\beta} \delta \mathbf{d}_{\Delta}) d\Omega \\ & + \int_{\Omega} [\Delta_{\alpha} \delta \mathbf{v} \cdot (\mathbf{G}_{\alpha} \Delta_{\alpha} \delta \mathbf{d}_{\Delta}) + \delta \mathbf{v} \cdot (\mathbf{H} \delta \mathbf{d}_{\Delta}) \\ & - \delta \mathbf{v} \cdot (\bar{\mathbf{L}} \delta \mathbf{d}_{\Delta})] d\Omega \\ & - \int_{\Gamma} \delta \mathbf{v} \cdot (\bar{\mathbf{L}}^{\Gamma} \delta \mathbf{d}_{\Delta}) d\Gamma, \end{aligned} \tag{123}$$

where $\mathbf{D}_{\alpha\beta}^{\text{alg}}$ is given in (119), \mathbf{G}_{α} is given by

$$\mathbf{G}_{\alpha} = \begin{bmatrix} \mathbf{O} & \mathbf{O} & -\frac{1}{2} \text{Skew}(\mathbf{Q}_{i+1} \mathbf{n}_{\alpha m}^r) \boldsymbol{\Xi}_{\Delta} \\ \mathbf{O} & \mathbf{O} & \mathbf{W}^T(\boldsymbol{\alpha}_{\Delta}, \mathbf{Q}_{i+1} \mathbf{m}_{\alpha m}^r) \\ \frac{1}{2} \text{Skew}(\mathbf{Q}_{1/2} \mathbf{n}_{\alpha m}^r) & \mathbf{O} & \frac{1}{2} \mathbf{Z}_{1/2, \alpha} \text{Skew}(\mathbf{Q}_{i+1} \mathbf{n}_{\alpha m}^r) \boldsymbol{\Xi}_{\Delta} \end{bmatrix} \tag{124}$$

and

$$\mathbf{H} = \frac{\partial \dot{\mathbf{g}}_m}{\partial \mathbf{d}_{\Delta}} = \begin{bmatrix} \mathbf{H}_u & \mathbf{O} \\ \mathbf{O} & \mathbf{H}_{\alpha} \end{bmatrix}, \quad \bar{\mathbf{L}} = \frac{\partial \bar{\boldsymbol{\sigma}}_m}{\partial \mathbf{d}_{\Delta}}, \quad \text{and} \quad \bar{\mathbf{L}}^{\Gamma} = \frac{\partial \bar{\boldsymbol{\sigma}}_m^{\Gamma}}{\partial \mathbf{d}_{\Delta}}, \tag{125}$$

with

$$\begin{aligned} \mathbf{H}_u &= \frac{2}{\Delta t^2} \bar{\mathbf{M}} \mathbf{I} \quad \text{and} \\ \mathbf{H}_{\alpha} &= \frac{2}{\Delta t^2} \mathbf{Q}_{1/2} \left[\bar{\mathbf{J}}^r + \frac{1}{2} A_{\Delta}^r \bar{\mathbf{J}}^r - \frac{1}{2} \text{Skew}(\bar{\mathbf{J}}^r \boldsymbol{\alpha}_{\Delta}^r) \right] \mathbf{Q}_i^T \\ & - \frac{1}{\Delta t^2} \text{Skew} \left\{ \mathbf{Q}_{i+1} \left[\bar{\mathbf{J}}^r(\boldsymbol{\alpha}_{\Delta}^r - \Delta t \boldsymbol{\omega}_i^r) + \frac{1}{2} \boldsymbol{\alpha}_{\Delta}^r \times \bar{\mathbf{J}}^r \boldsymbol{\alpha}_{\Delta}^r \right] \right\} \boldsymbol{\Xi}_{\Delta}. \end{aligned} \tag{126}$$

6 Finite element implementation and numerical examples

The six-node triangular element of [5] is adopted as the basis for our finite element implementations. The element is purely displacement-based and is equipped with quadratic interpolations for the incremental displacements \mathbf{u}_{Δ} and linear interpolations for the incremental rotations $\boldsymbol{\alpha}_{\Delta}$, these latter being placed on the mid-side nodes only.

Let \mathbf{p}_{Δ} and $\delta \mathbf{p}_{\Delta}$ be the element vectors that collect these nodal degrees-of-freedom and their variations, and let \mathbf{N} be the matrix of element shape functions. With these definitions, finite element approximations of Galerkin type are written as

$$\mathbf{d}_{\Delta} = \mathbf{N} \mathbf{p}_{\Delta}, \quad \delta \mathbf{d}_{\Delta} = \mathbf{N} \delta \mathbf{p}_{\Delta} \quad \text{and} \quad \delta \mathbf{v} = \mathbf{N} \delta \mathbf{p}_{\Delta}. \tag{127}$$

Introducing (127) into (105), we obtain the element residual force vector as follows

$$\begin{aligned} \mathbf{P} = & \int_{\Omega} [(\Delta_{\alpha} \mathbf{N})^T \Phi_{\alpha 1/2}^T \Lambda_m \boldsymbol{\sigma}_{\alpha m}^r + \mathbf{N}^T \dot{\mathbf{g}}_m - \mathbf{N}^T \bar{\boldsymbol{\sigma}}_m] d\Omega \\ & - \int_{\Gamma} \mathbf{N}^T \bar{\boldsymbol{\sigma}}_m^{\Gamma} d\Gamma, \end{aligned} \tag{128}$$

and from (127) into (123) we obtain the element stiffness matrix

$$\begin{aligned} \mathbf{k} = & \int_{\Omega} [(\Delta_{\alpha} \mathbf{N})^T \Phi_{\alpha 1/2}^T \Lambda_m \mathbf{D}_{\alpha\beta}^{\text{alg}} \Lambda_{i+1}^T \Phi_{\beta i+1} Y_{\beta \Delta} (\Delta_{\beta} \mathbf{N})] d\Omega + \\ & + \int_{\Omega} [(\Delta_{\alpha} \mathbf{N})^T \mathbf{G}_{\alpha} (\Delta_{\alpha} \mathbf{N}) + \mathbf{N}^T \mathbf{H} \mathbf{N} - \mathbf{N}^T \bar{\mathbf{L}} \mathbf{N}] d\Omega \\ & - \int_{\Gamma} \mathbf{N}^T \bar{\mathbf{L}}^{\Gamma} \mathbf{N} d\Gamma. \end{aligned} \tag{129}$$

Within a Newton solution procedure, we must compute, at every iteration, the following quantities at t_{i+1} , from their values at t_i and from the current values of \mathbf{u}_{Δ} and $\boldsymbol{\alpha}_{\Delta}$:

$$\begin{aligned} \dot{\mathbf{u}}_{i+1} &= \frac{2}{\Delta t} \mathbf{u}_{\Delta} - \dot{\mathbf{u}}_i, & \dot{\boldsymbol{\omega}}_{i+1} &= \frac{4}{\Delta t^2} \boldsymbol{\alpha}_{\Delta} - \mathbf{Q}_{\Delta} \left(\frac{4}{\Delta t} \boldsymbol{\omega}_i + \dot{\boldsymbol{\omega}}_i \right), \\ \ddot{\mathbf{u}}_{i+1} &= \frac{4}{\Delta t^2} \mathbf{u}_{\Delta} - \frac{4}{\Delta t} \dot{\mathbf{u}}_i - \ddot{\mathbf{u}}_i, & \boldsymbol{\kappa}_{i+1}^r &= \boldsymbol{\kappa}_{\alpha i}^r + \Delta \boldsymbol{\kappa}^r, \\ \boldsymbol{\omega}_{i+1} &= \frac{2}{\Delta t} \boldsymbol{\alpha}_{\Delta} - \mathbf{Q}_{\Delta} \boldsymbol{\omega}_i, & \boldsymbol{\alpha}_{i+1} &= \frac{4}{4 - \boldsymbol{\alpha}_{\Delta} \cdot \boldsymbol{\alpha}_i} \\ & & & (\boldsymbol{\alpha}_{\Delta} + \boldsymbol{\alpha}_i + \frac{1}{2} \boldsymbol{\alpha}_{\Delta} \times \boldsymbol{\alpha}_i). \end{aligned} \tag{130}$$

After convergence, the following updates must be performed at every node

$$\mathbf{u} \leftarrow \mathbf{u} + \mathbf{u}_{\Delta} \quad \text{and} \quad \mathbf{u}_{\Delta} = \boldsymbol{\alpha}_{\Delta} = \mathbf{0}, \tag{131}$$

whereas at each integration point we must set

$$\begin{aligned} \dot{\mathbf{u}}_i &\leftarrow \dot{\mathbf{u}}_{i+1}, & \dot{\boldsymbol{\omega}}_i &\leftarrow \dot{\boldsymbol{\omega}}_{i+1}, \\ \ddot{\mathbf{u}}_i &\leftarrow \ddot{\mathbf{u}}_{i+1}, & \boldsymbol{\kappa}_{\alpha i}^r &\leftarrow \boldsymbol{\kappa}_{i+1}^r, \\ \boldsymbol{\omega}_i &\leftarrow \boldsymbol{\omega}_{i+1}, & \boldsymbol{\alpha}_i &\leftarrow \boldsymbol{\alpha}_{i+1}. \end{aligned} \tag{132}$$

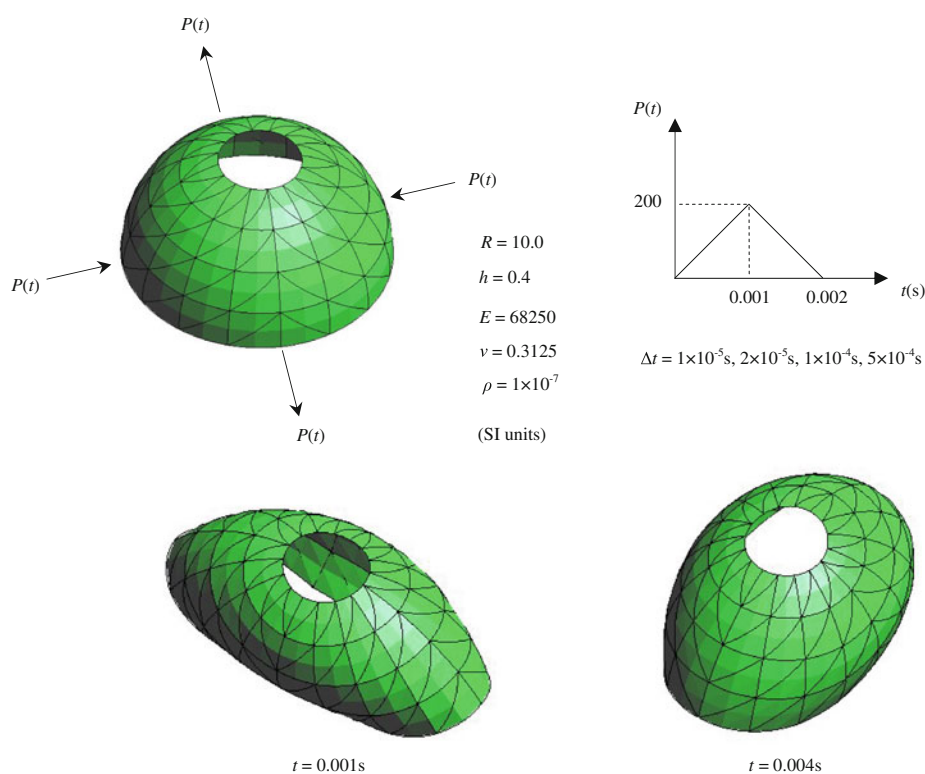
In the following sections, we assess the performance of the developed formulation by means of several numerical examples. Full numerical integration using 3 Gauss points is performed for computation of the elements matrices and vectors, together with 3 Gauss points for integration across the thickness. No special techniques such as ANS or EAS are employed since the element does not suffer from any locking misbehavior in the thin-shell limit (see [5]). Computation of the scalar parameter ϑ is performed locally at the integration points, hence ϑ is always eliminated at the element level.

Remark As we work with the three components of the rotation vector, there is no need for special connection schemes on shell intersections and on connections with rod elements, stiffeners and rigid bodies. However, a fictitious stiffness needs to be added to the drilling rotation or, equivalently, a fictitious inertia component must be introduced into $\bar{\mathbf{J}}^r$. We adopt here the value of Eh^3 for the fictitious stiffness ($E =$ elasticity modulus; $h =$ shell thickness), based on the work of [6] and also on the very good results we have experienced in [5, 13, 14, 16] for static problems. Differently from statics, however, we found that this degree of freedom deserves a little more attention in dynamics. Depending on the physical nature of a problem—whether being dominated by elastic or inertia forces—the fictitious value added to the FEM tangent matrix may (slightly) affect the results. For instance, we found that by varying the stiffness value from $10^{-2}Eh^3$ to 10^4Eh^3 , the energy level of a system can be (even though to a small degree) affected if the problem is dominated by elastic

forces. Analogously, by adopting a fictitious inertia component on $\bar{\mathbf{J}}^r$ instead of using the fictitious stiffness, there may also happen some consequences in the energy level if the system is dominated by inertia forces. This aspect deserves a thorough investigation on a comprehensive set of examples, and this is currently being carried out (conclusions will be drawn on a future paper). Approaches that use only two rotational degrees-of-freedom or that circumvent the use of rotational variables within the context of conserving dynamics are also possible (see e.g. [4] and references therein), but this is not the aim of our work.

It is also important to draw a few comments on the objectivity issue within our formulation. The shell theory presented in Sect. 3 entirely fulfills objectivity requirements in the sense of [2, 3, 9, 10, 18, 22]. The strain and stress measures are defined as material (back-rotated) quantities and thus render invariant under superposed rigid body motions. However, discretizations of finite element type such as (127) are usually claimed to destroy the objectivity of the strains at interior points of the elements. In this sense, we would like to recall that we make use of an updated formulation (i.e. the incremental rotations are interpolated and not the total rotations), and that the rotation vector α_i and the curvature strains $\kappa_{\alpha i}^r$ from the last converged step are stored *at the integration points*: they do not need to be computed from the nodal rotations. For this reason, rigid body rotations can be easily superposed to the deformed shell at any time instant by applying $\alpha_\Delta = \bar{\alpha}_\Delta = constant$

Fig. 2 Free vibration of hemispherical shell. Problem data



directly at every node. We refer to our remark on this question on Sect. 6 of Part 1.

6.1 Free vibration of a hemispherical shell

In this first example we want to validate our algorithm for the case of linear-elastic materials by comparing our results with a reference solution. For this purpose, let us consider the hemispherical shell of Fig. 2, which was analyzed in [19]. The geometric and material properties are as shown in the figure. Two pairs of concentrated forces are applied until $t = 2.0$ ms, after which they are removed and the structure undergoes a free vibration motion. We discretize the problem by using four element divisions per quadrant on both radial and circumferential directions, with no consideration of symmetry conditions. The results obtained for the displacements under the load points with $\Delta t = 10^{-5}$ s are depicted in Fig. 3, together with the energy (internal plus kinetic) graph where exact conservation can be found. Deformed shapes are shown at the bottom of Fig. 2; no amplification factor is adopted. We remark that our displacement solution shows a vibration motion with constant amplitude in time, what is not observed in the results reported by [19] using the same time increment. We also remark that, by using time steps as large as two orders of magnitude higher, the same smooth and stable solution is attained, with the very same amplitude of displacements and energy conservation properties. We found this to be an outstanding performance of the algorithm.

6.2 Dynamics of a tumbling cylinder

Let us consider now the example proposed in [21] that deals with the dynamics of a linear-elastic cylindrical shell, with material properties and initial geometry as shown in Fig. 4. Here we present a different version of the problem and assume that the cylinder is made of a neo-Hookean hyper-elastic material of the type defined in Eq. (53). Starting at rest, the cylinder is subjected to four sets of nodal loadings applied at positions 90° apart from each other, whose time-history is shown in Fig. 4. The loads vanish at $t = 1.0$ s, leading the structure to a complex free motion in which the total energy and both momenta must be exactly conserved. In each of the loading positions, the loads are applied as nodal loads on all nodes along height H (values indicated in Fig. 4 stand for the resultant force acting on that direction at each position). Figure 5 shows the time histories of energy (internal plus kinetic) and angular momentum obtained using all time steps adopted. The motion of the cylinder is also illustrated by a sequence of deformed shapes with no magnification factor.

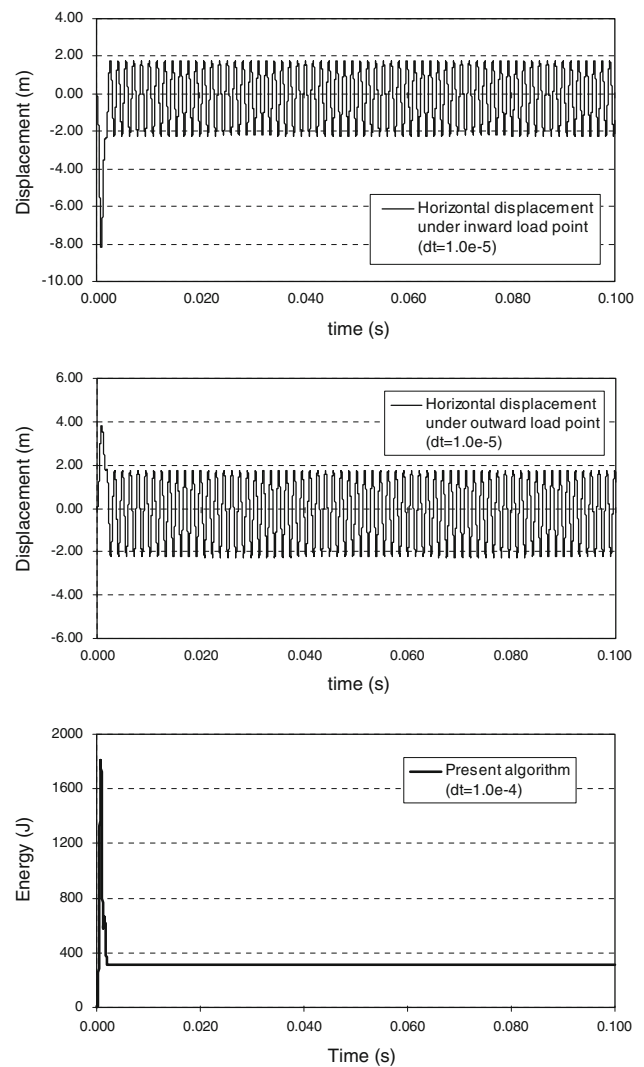


Fig. 3 Free vibration of hemispherical shell. Analysis results

6.3 Dynamics of a satellite-like structure

This interesting problem was first proposed in [21] and deals with the dynamics of a satellite-like structure made up of three intersecting plates, as shown in Fig. 6. The structure is at rest in the beginning of the motion and is subjected to a system of uniformly distributed loads at the free edges, whose pattern follows a hat function in time. The loads are removed at $t = 1.0$ s and then a free motion with vibration takes place, in which both momenta and energy must be preserved. The distributed loadings are applied here as nodal loads at all nodes laying on the free edges (values indicated in Fig. 6 correspond to the resultant force acting on each direction of the edges). Differently from [21], where the material is assumed to be linear elastic, we adopt here a neo-Hookean material of the type defined in (53). Figure 7 depicts time-histories of energy (internal plus kinetic) and angular

Fig. 4 Dynamics of a tumbling cylinder. Problem data

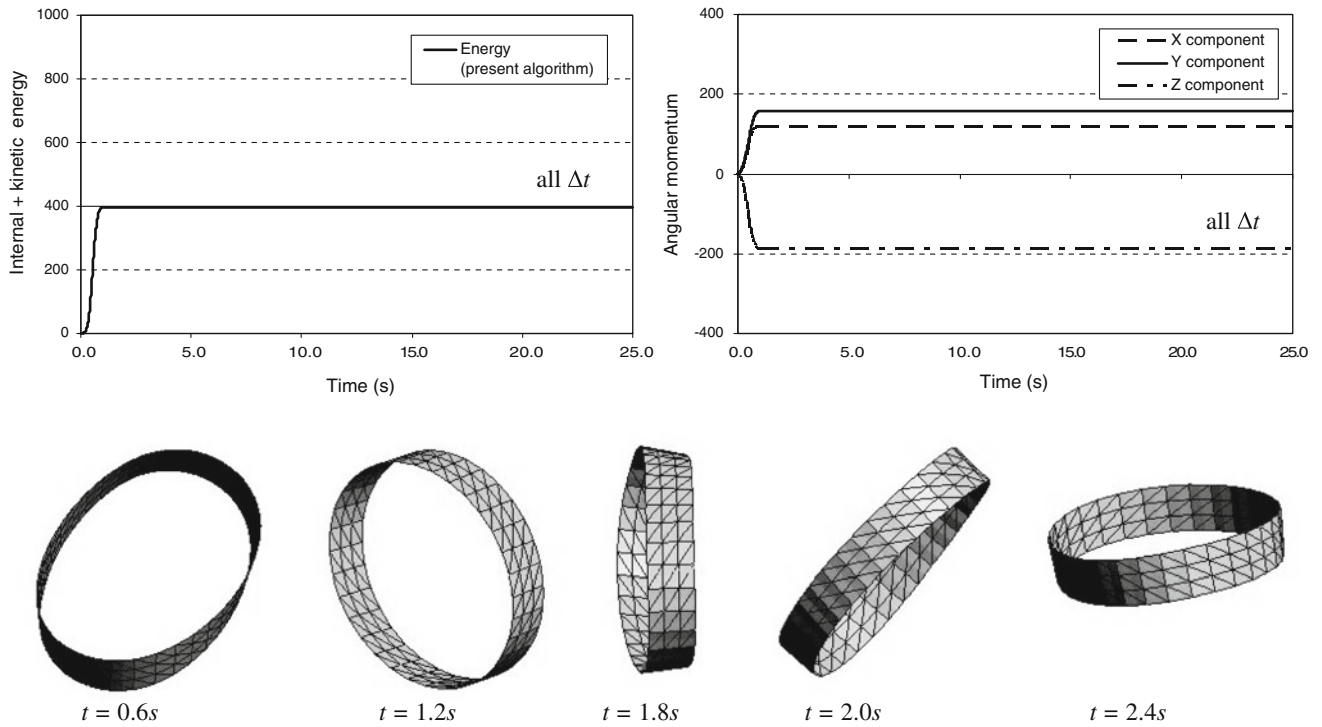
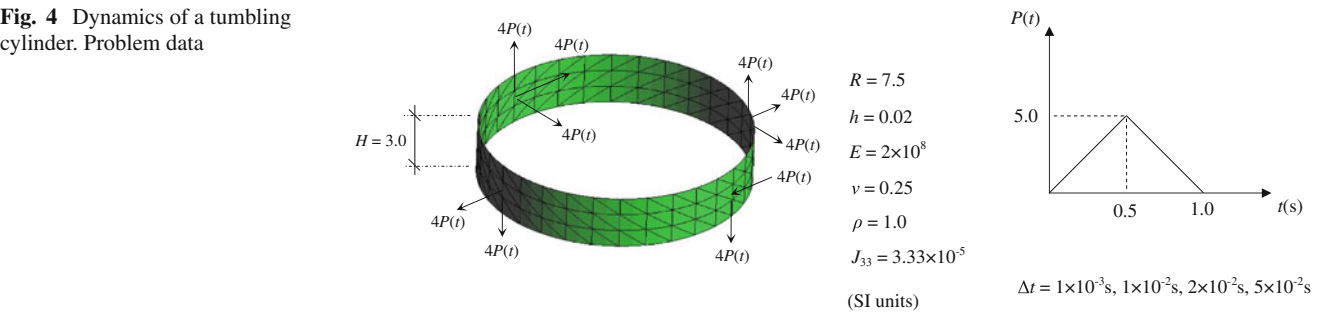
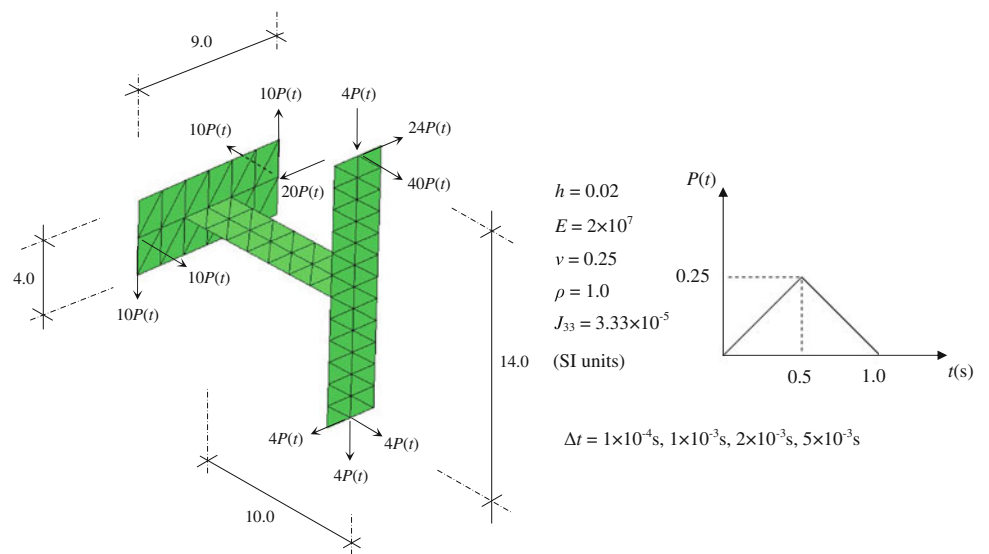


Fig. 5 Dynamics of a tumbling cylinder. Analysis results

Fig. 6 Dynamics of a satellite-like structure. Problem data



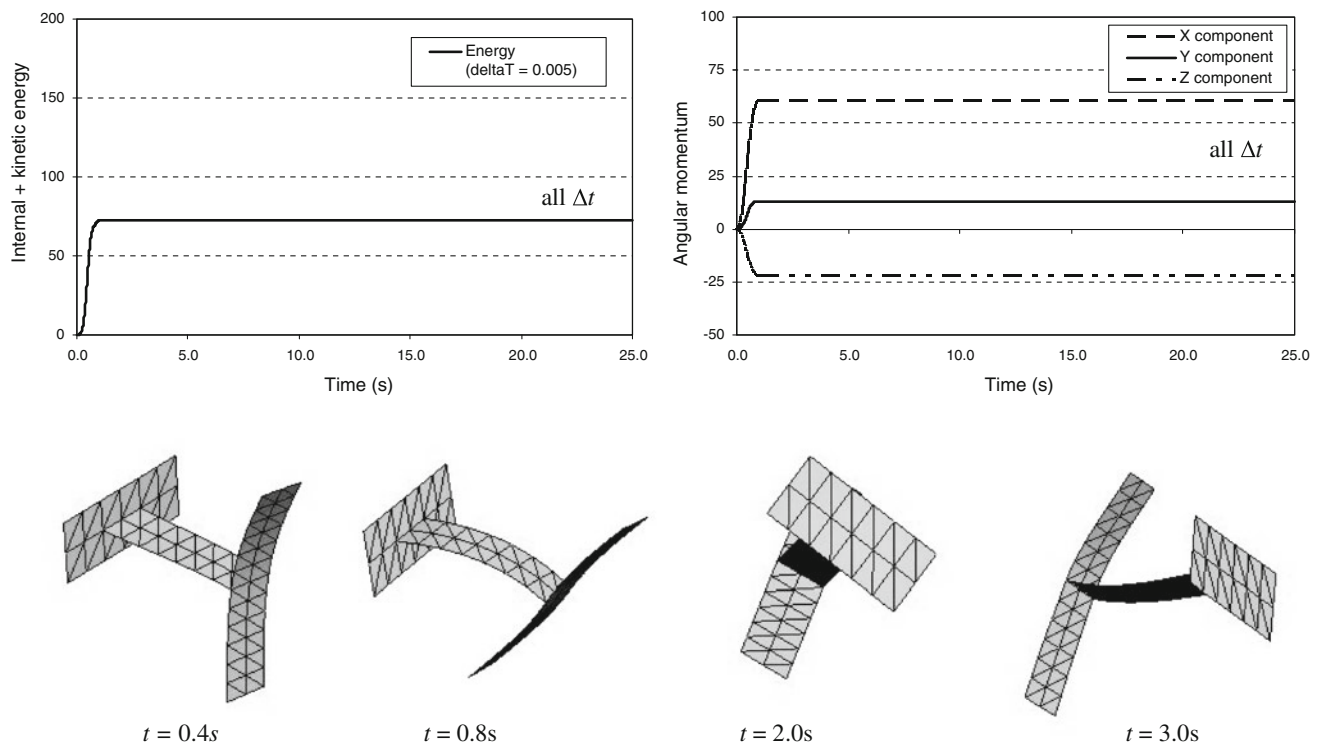


Fig. 7 Dynamics of a satellite-like structure. Analysis results

momentum, together with a plot of selected deformed configurations. Analysis of the problem using a linear-elastic material leads to the same results reported in [21].

It is worth mentioning that a careful investigation of this example has been performed recently in [7], where a different value for the system energy after $t = 1.0$ s is attained. The source of this discrepancy is reported to be in the way that the loads are interpreted, once the description of this loading is problematic in the literature: there is no consent as to whether the values shown in [21] are for a uniformly distributed loading or for nodal point forces. In reference [7], the authors assume that the loads shown are per unit length of the edges. Similar interpretation was made in [4]. In our work, we follow the load assumptions from these two works and obtain the same energy response as in [21]. Namely, the energy level remains at the value of nearly 70 after the loads are removed. We should report, however, that by increasing the value of the fictitious drilling stiffness in the analyses, the energy level approaches the one obtained in [7] (which is at about 60).

7 Conclusions

A fully conserving algorithm was derived in this paper for the integration of the equations of motion in nonlinear

shell dynamics. The resulting expressions are nearly identical to the ones of the rod model of Part 1 of this work, allowing for a straightforward implementation of the shell dynamics within a finite element code once the rod model has been implemented. The Rodrigues rotation vector was adopted to describe the rotation field; as a consequence, update of the rotational variables became extremely simple. Following an energy-momentum approach, a special time-collocation scheme was devised for the weak form, and conservation of both momentum and total energy in the absence of external forces was attained within the algorithm. It is worth noting that the special choice of the weighting functions in the construction of the algorithmic weak form led to a very simple expression for the enforcement of energy conservation. Appealing is the fact that general hyperelastic materials were permitted in a totally consistent way, and we believe this is our major contribution in the context of nonlinear dynamics of shells with rotational degrees-of-freedom. Validity and robustness of the formulation were shown by means of three numerical simulations.

Acknowledgments E.M.B. Campello acknowledges fellowship funding from CNPq (*Conselho Nacional de Desenvolvimento Científico e Tecnológico*, grant number 305869/2009-4) and FAPESP (*Fundação de Amparo à Pesquisa do Estado de São Paulo*, grant number 05/52453-2), as well as material support from IBNM (Institute of Mechanics and

Computational Mechanics, Leibniz University of Hanover) during a post-doc stay in Hanover. P.M. Pimenta acknowledges the *Mercator Gastprofessur* from DFG (*Deutsche Forschungsgemeinschaft*) that made possible his stay at the IBNM on a leave from the University of São Paulo, as well as the support from CNPq under the grant 305822/2006-3.

References

- Argyris JH (1982) An excursion into large rotations. *Comput Methods Appl Mech Eng* 32:85–155
- Bertram A (2005) Elasticity and plasticity of large deformations—an introduction. Springer, Berlin
- Betsch P, Steinmann P (2002) Frame-indifferent beam finite elements based upon the geometrically-exact beam theory. *Int J Numer Methods Eng* 54:1775–1788
- Betsch P, Sanger N (2009) On the use of geometrically exact shells in a conserving framework for flexible multibody dynamics. *Comput Methods Appl Mech Eng* 198:1609–1630
- Campello EMB, Pimenta PM, Wriggers P (2003) A triangular finite shell element based on a fully nonlinear shell formulation. *Comput Mech* 31:505–518
- Chrosielewski J, Makowski J, Stumpf H (1992) Genuinely resultant shell finite elements accounting for geometric and material non-linearity. *Int J Numer Methods Eng* 35:63–94
- Chrosielewski J, Witkowski W (2010) Discrepancies of energy values in dynamics of three intersecting plates. *Int J Numer Methods Biomed Eng* 26:1188–1202
- Ciarlet PJ (1988) *Mathematical elasticity*, vol 1. North Holland, Amsterdam
- Crisfield MA, Jelenic G (1999) Objectivity of strain measures in the geometrically-exact three-dimensional beam theory and its finite element implementation. *Proc R Soc Lond* 455:1125–1147
- Ibrahimbegovic A, Taylor RL (2002) On the role of frame-invariance in structural mechanics models at finite rotations. *Comput Methods Appl Mech Eng* 191:5159–5176
- Laursen TA, Meng XN (2001) A new solution procedure for application of energy-conserving algorithms to general constitutive models in nonlinear elastodynamics. *Comput Methods Appl Mech Eng* 190:6309–6322
- Pimenta PM (1993) On a geometrically-exact finite strain shell model. In: *Proceedings of the 3rd Pan-American Congress on applied mechanics*, III PACAM, So Paulo
- Pimenta PM, Campello EMB, Wriggers P (2004) A fully nonlinear multi-parameter shell model with thickness variation and a triangular shell finite element. *Comput Mech* 34:181–193
- Pimenta PM, Campello EMB (2005) Finite rotation parameterizations for the nonlinear static and dynamic analysis of shells. In: Ramm E, Wall WA, Bletzinger K-U, Bischoff M (eds) *Proceedings of the 5th international conference on computation of shell and spatial structures*, Salzburg, Austria
- Pimenta PM, Campello EMB, Wriggers P (2008) An exact conserving algorithm for nonlinear dynamics with rotational DOFs and general hyperelasticity. Part 1: Rods. *Comput Mech* 42:715–732
- Pimenta PM, Campello EMB (2009) Shell curvature as an initial deformation: a geometrically exact finite element approach. *Int J Numer Methods Eng* 78:1094–1112
- Rodrigues O (1840) Des lois geometriques qui regissent les deplacements d’un systeme solide dans l’espace, et de la variation des coordonnees provenant de ces deplacements consideres independamment des causes qui peuvent les produire. *J Math Pure Appl* 380–440
- Romero I, Armero F (2002) An objective finite element approximation of the kinematics of geometrically-exact rods and its use in the formulation of an energy-momentum conserving scheme in dynamics. *Int J Numer Methods Eng* 54:1683–1716
- Sansour C, Wriggers P, Sansour J (1997) Nonlinear dynamics of shells: theory, finite element formulation and integration schemes. *Nonlinear Dyn* 13:279–305
- Simo JC, Tarnow N (1992) The discrete energy-momentum method. Conserving algorithms for nonlinear elastodynamics. *Z Angew Math Phys* 43:757–792
- Simo JC, Tarnow N (1994) A new energy and momentum conserving algorithm for the nonlinear dynamics of shells. *Int J Numer Methods Eng* 37:2527–2549
- Truesdell C (1965) *Continuum mechanics*, vols 1–4. Gordon and Breach, New York
- Wood WL, Bossak M, Zienkiewicz OC (1981) An alpha modification of Newmark’s method. *Int J Numer Methods Eng* 15:1562–1566